

## Supporting Information

### **A highly selective and sensitive fluorescent probe for simultaneously distinguishing and sequentially detecting hydrogen multiple thiol species in solution and in live cells**

Dan Qiao<sup>a</sup>, Tangliang Shen<sup>a</sup>, Mengyuan Zhu<sup>b</sup>, Xiao Liang<sup>a</sup>, Lu Zhang<sup>a</sup>, Zheng Yin<sup>a</sup>, Binghe Wang<sup>b\*</sup>, Luqing Shang<sup>a\*</sup>

*a. College of Pharmacy & State Key Laboratory of Elemento-Organic Chemistry, Nankai University Tianjin 300071 (P.R. China) E-*

*mail: shanglq@nankai.edu.cn*

*b. Department of Chemistry Georgia State University Atlanta, Georgia 30303 USA E-mail: wang@gsu.edu*

## **Experimental Section**

### **1. Apparatus**

<sup>1</sup>H-NMR (400 MHz) and <sup>13</sup>C-NMR (100 MHz) spectra were recorded on a Bruker AVANCE-400 (400 MHz) (Bruker, Karlsruhe, Germany) NMR spectrometer and TMS as an internal standard. Electrospray ionization mass spectroscopy (ESI-MS) was performed on a Shimadzu LC/MS-2020 (Shimadzu, Kyoto, Japan). HRMS were recorded on a high-resolution ESI-FTICR mass spectrometer (Varian 7.0 T, Varian, USA). UV-vis spectra were measured by a UH-5300 spectrophotometer (Hitachi). Fluorescence measurements were recorded on a F-7000 spectrophotometer (Hitachi). Fluorescence images of cells were taken by a laser scanning confocal microscopy (Leica TCS SP8).

### **2. Materials**

Unless otherwise stated, all reagents used in this study were commercial products without further purification. Twice-distilled water was used throughout all experiments. TLC analysis was performed on silica gel plates and column chromatography was conducted over silica gel (mesh 200 - 300), both of which were obtained from the Qingdao Ocean Chemicals. Mito-Tracker Green was obtained from Solarbio.

### **3. Detection limit**

The limit of detection defined by  $3\sigma/k$ , where  $\sigma$  is the standard deviation of the blank sample and  $k$  is the slope of the linear regression equation.

### **4. Theoretical study on the fluorescence mechanism**

The structure of **NCR** was constructed using Gaussian<sup>1</sup>, which was initially optimized using the capabilities within these aforementioned programs. Calculations were then conducted using density functional theory (DFT) with the B3LYP<sup>2</sup> exchange functional employing 6-31G(d)<sup>3</sup> level implemented via the Gaussian 09 suite of programs for the full geometry optimization and frequency calculations of the probe. Imaginary frequencies were not obtained in any of the frequency calculations.

### **5. Cells culture**

HeLa cells were cultured in DMEM (Dulbecco's modified Eagle's medium) and supplemented with 10% FBS (fetal bovine serum), penicillin (100 µg/mL) and streptomycin (100 µg/mL) in an atmosphere of 5% CO<sub>2</sub> and 95% air at 37 °C.

### **6. MTT assay**

Cell cytotoxicity was evaluated by MTT assay. Cells were cultivated in a 96-well plate until 50-70% confluence, and then incubated with different concentrations of **NCR** (0-20  $\mu\text{M}$ ) for 24 h. 20  $\mu\text{L}$  3-(4,5-dimethyl-2-thiazolyl)-2,5-diphenyltetrazolium bromide (MTT, 5 mg/ mL) was added for 4 h at 37  $^{\circ}\text{C}$ . After removing the MTT, 100  $\mu\text{L}$  DMSO was added. The absorbance intensities at 570 nm were measured using a plate reader. All experiments were repeated five times, and the data were presented as the percentage of control cells.

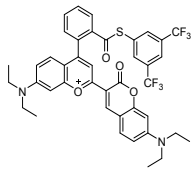
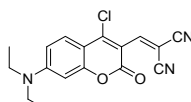
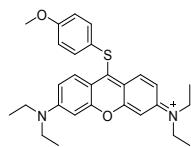
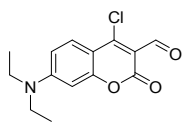
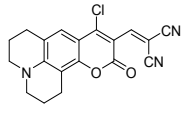
### **7. Discriminative fluorescence imaging of biothiols in live cells**

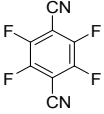
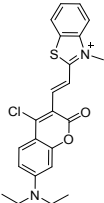
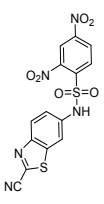
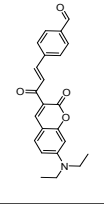
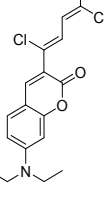
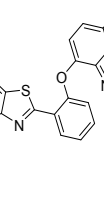
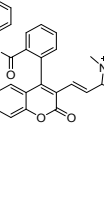
The cell experiment was divided into six groups. In the first group, HeLa cells were incubated with **NCR** (5  $\mu\text{M}$ ) for 30 min and imaged after washing by phosphate-buffered saline (PBS) for three times. For the second group, HeLa cells were pretreated with NEM (0.5 mM) for 30 min, subsequently incubated with **NCR** (5  $\mu\text{M}$ ) for 30 min, and then washed by PBS buffer for three times before imaging. In the third to sixth group, HeLa cells were pretreated with NEM (0.5 mM) for 30 min, subsequently incubated with NaHS/Cys/Hcy/GSH (500  $\mu\text{M}$ , 30 min) and probe **NCR** (5  $\mu\text{M}$ , 30 min), and then washed with PBS buffer for three times. Cells were imaged by a laser scanning confocal microscopy (Leica TCS SP8;  $\lambda_{\text{ex}} = 405 \text{ nm}$ ,  $\lambda_{\text{em}} = 440\text{-}490 \text{ nm}$  for the blue channel;  $\lambda_{\text{ex}} = 561 \text{ nm}$ ,  $\lambda_{\text{em}} = 575\text{-}620 \text{ nm}$  for the red channel).

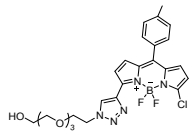
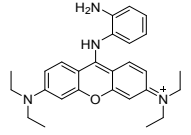
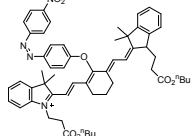
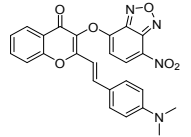
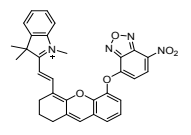
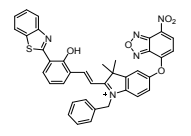
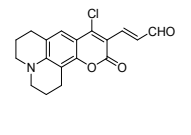
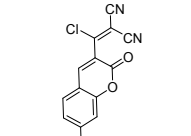
### **8. Sequential fluorescence imaging of biothiols in live cells**

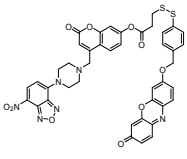
The cell experiment was divided into four groups. In the first group, HeLa cells were pretreated with NEM (0.5 mM) for 30 min, subsequently incubated with **NCR** (5  $\mu\text{M}$ ) for 30 min, and then imaged after washing three times by PBS buffer, as the control group. In the second to fourth group, HeLa cells were pretreated with NEM (0.5 mM) for 30 min, subsequently incubated with Cys /Hcy/GSH (500  $\mu\text{M}$ ) for 30 min, washed and continued to be incubated with **NCR** (5  $\mu\text{M}$ ) for 30 min, and then added 500  $\mu\text{M}$  NaHS to the culture dish, after 30 min, imaged after washing three times by PBS buffer. Cells were imaged by a laser scanning confocal microscopy (Leica TCS SP8;  $\lambda_{\text{ex}} = 405 \text{ nm}$ ,  $\lambda_{\text{em}} = 440\text{-}490 \text{ nm}$  for the blue channel;  $\lambda_{\text{ex}} = 561 \text{ nm}$ ,  $\lambda_{\text{em}} = 575\text{-}620 \text{ nm}$  for the red channel).

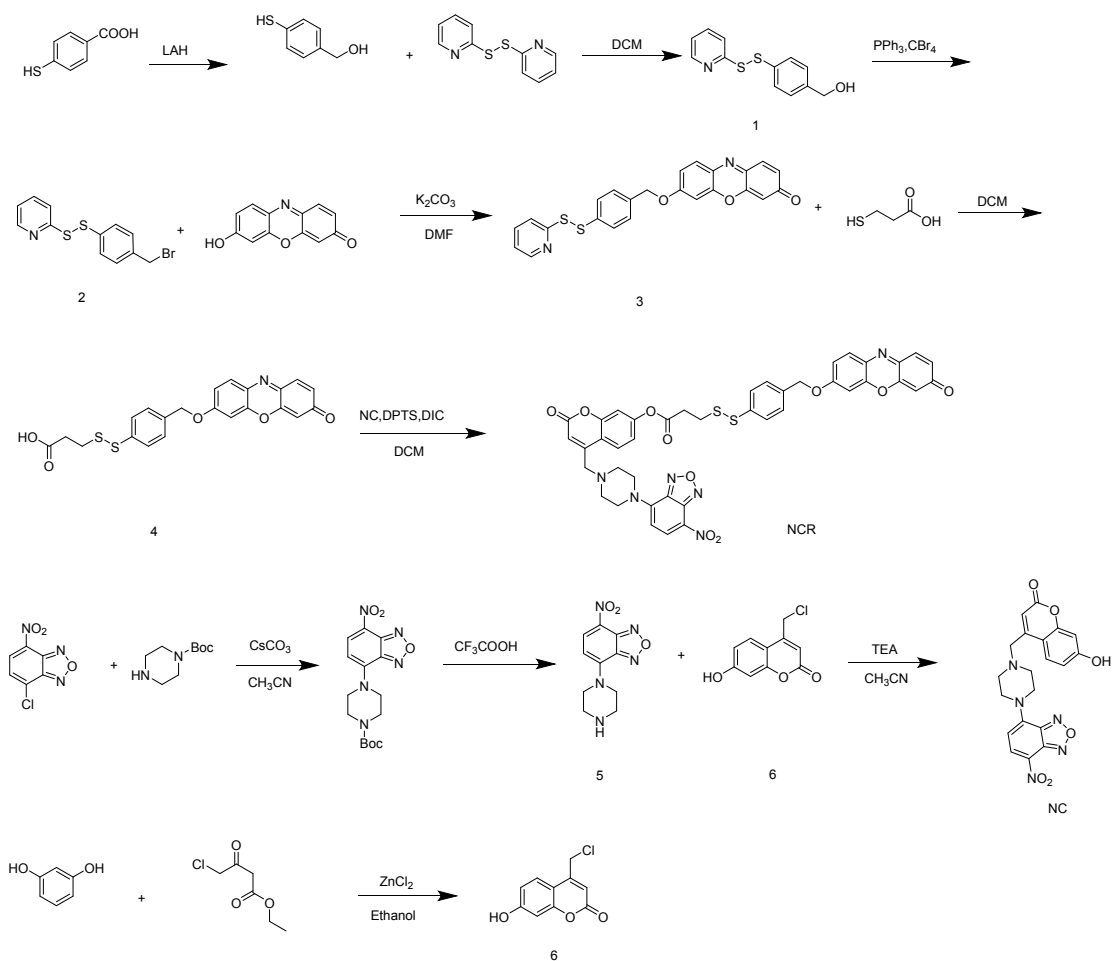
**Table S1.** Summary of the optical properties of representative fluorescent probes for distinguishing biothiols with multiple sets of fluorescence signals.

Multisite probe	Distinguishing targets for detection	Number of emission bands	Emission wavelength/nm	Emission distance/nm	Solubility	Targeting mitochondria	References
	Cys/Hcy	2	474,694	220	Ethanol/ PBS (40:60 v/v)	NO	4. <i>Anal. Chem.</i> , 2014, <b>86</b> ,1800- 1807
	GSH, H <sub>2</sub> S	2	517,564	47	DMF/P BS (3:7 v/v)	NO	5 <i>.Chem. Commun.</i> <i>(Camb.)</i> ,2016, <b>52</b> , 4628-4631.
	Cys/Hcy , GSH	2	546,622	76	PBS	NO	6. <i>Chem. Sci.</i> , 2014, <b>5</b> , 3183.
	Cys/Hcy , GSH	2	407/503, 546/503	33/43	PBS	NO	7. <i>Anal. Chim.</i> <i>Acta</i> ,2015, <b>900</b> , 103-110.
	Cys, GSH	2	500,560	60	CH <sub>3</sub> CN/ PBS (3:7 v/v)	NO	8. <i>Biosens.</i> <i>Bioelectron.</i> ,201 7, <b>90</b> ,117-124.

	Cys, Hcy, GSH	2	450,500	50	PBS	NO	9. <i>Chem. Sci.</i> , 2016, <b>7</b> ,256-260.
	Cys, GSH	2	420,512	92	PBS (1m M CTAB)	NO	10. <i>J. Am. Chem. Soc.</i> ,2014, <b>136</b> , 574-577.
	Cys, GSH	2	522,490	32	PBS	NO	11. <i>Anal. Chem.</i> , 2015, <b>87</b> ,3460-34 66.
	Cys, SO <sub>2</sub>	2	514,576	62	DMSO/ PBS (1:1 v/v)	NO	12. <i>J. Am. Chem. Soc.</i> , 2017, <b>139</b> , 3181-3185.
	GSH	1	505	-	DMSO/ PBS (1:1 v/v)	NO	13. <i>Sensors Actuators B: Chem.</i> , 2017, <b>253</b> ,42-49.
	H <sub>2</sub> S, Cys/Hcy , GSHp	2	465,550	85	DMSO/ PBS (1:4 v/v)	NO	14. <i>Sensors Actuators B: Chem.</i> , 2016, <b>235</b> ,691-697.
	Cys	2	494,644	150	DMF/P BS (1:9 v/v)	YES	15. <i>RSC Adv.</i> , 2014, <b>4</b> ,64542- 64550.

	Cys/Hcy , GSH	2	564,588	24	CH <sub>3</sub> CN/ HEPES (5:95 v/v)	NO	16. <i>J. Am. Chem. Soc.</i> ,2012, <b>134</b> ,1 8928-18931.
	Cys, GSH	2	536,618	82	CH <sub>3</sub> CN/ PBS (3:7 v/v)	YES	17. <i>J. Am. Chem. Soc.</i> ,2014, <b>136</b> ,1 2520-12523.
	Cys/Hcy , GSH	2	764,810	46	HEPES	YES	18. <i>J. Am. Chem. Soc.</i> ,2014, <b>136</b> , 7018-7025.
	Cys/Hcy , GSH	2	545,621	76	CH <sub>3</sub> CN/ HEPES (3:7 v/v)	NO	19. <i>Anal. Chem.</i> , 2016, <b>88</b> ,3638-36 46.
	Cys/Hcy , GSH	2	550,716	166	DMSO/ PBS (5:95 v/v)	NO	20. <i>Biosens. Bioel ectron.</i> ,2016, <b>81</b> , 341-348.
	H <sub>2</sub> S, Cys/Hcy , GSH	3	485,546,6 09	61/63	CH <sub>3</sub> CN/ PBS (2:8 v/v)	YES	21. <i>Chem. Sci.</i> , 2017, <b>8</b> ,6257-626 5.
	Cys, Hcy	2	480,542	62	DMSO/ PBS (2:8 v/v)	NO	22. <i>Chem. Asian J.</i> , 2017, <b>12</b> , 2098-2103.
	Cys, Hcy, GSH	3	457,559,5 29	72/30	DMSO/ PBS (6:4 v/v)	NO	23. <i>Angew. Chem. Int. Ed.</i> ,2018, <b>57</b> ,4 991-4994.

	<p>H<sub>2</sub>S, Cys/ Hcy, GSH</p>	<p>2</p>	<p>467/588</p>	<p>121</p>	<p>DMSO/ PBS (1:99 v/v)</p>	<p>YES</p>	<p>This work</p>
-----------------------------------------------------------------------------------	--------------------------------------------------	----------	----------------	------------	-----------------------------------------	------------	------------------



**Scheme S1.** The synthetic route of probe NCR.

**Synthesis of 2.** Compound **1** was prepared via previous method<sup>24</sup>. Triphenylphosphine (632 mg, 2.4 mmol) and carbon tetrabromide (800 mg, 2.4 mmol) were dissolved absolutely in dichloromethane. Compound **1** (400 mg, 1.6 mmol) was slowly added. TLC was applied to monitor the reaction. After complete reaction, the solvent was evaporated under reduced pressure. The resulted residue was purified by silica gel column chromatography with PE/EA (v/v 100:1) to give a yellow oil as compound **2** (200 mg, 40%).

**Synthesis of 3.** Resorufin (136.6 mg, 0.64 mmol) and potassium carbonate (132.7 mg, 0.96 mmol) were dissolved absolutely in dry DMF. Under the protection of nitrogen, compound **2** (200 mg, 0.64 mmol) was slowly added. The mixture was stirred for overnight at 55 °C. After complete reaction, 50 mL water was added into the flask and the reaction mixture was extracted with EA (100 mL × 3). The organic phase was



collected and dried using MgSO<sub>4</sub>. Then the solvent was removed under reduced pressure affording the crude product, which was purified by flash chromatography column using CH<sub>2</sub>Cl<sub>2</sub>/MeOH (v/v = 250:1) to afford red solid as compound **3** (210 mg, 73%).

<sup>1</sup>H NMR (400 MHz, CDCl<sub>3</sub>) δ 8.47 (s, 1H), 7.70 (d, *J* = 8.8 Hz, 1H), 7.66 – 7.54 (m, 4H), 7.39 (t, *J* = 9.6 Hz, 3H), 7.11 (s, 1H), 6.98 (d, *J* = 8.9 Hz, 1H), 6.83 (d, *J* = 10.6 Hz, 2H), 6.31 (s, 1H), 5.13 (s, 2H). <sup>13</sup>C NMR (101 MHz, CDCl<sub>3</sub>) δ 186.3, 162.3, 159.3, 149.8, 149.7, 145.8, 145.6, 137.3, 136.8, 134.7, 134.6, 134.3, 131.6, 128.6, 128.3, 127.6, 121.1, 119.7, 114.2, 106.8, 101.1, 70.3. HRMS: *m/z* [M+Na]<sup>+</sup> calculated for C<sub>24</sub>H<sub>16</sub>N<sub>2</sub>NaO<sub>3</sub>S<sub>2</sub>: 467.0495; measured 467.0497.

**Synthesis of 4.** Compound **3** (210 mg, 0.47 mmol) was dissolved absolutely in dichloromethane. 3-Mercaptopropionic acid (60.4 mg, 0.57 mmol) was slowly added. The reaction was monitored by TLC. After complete reaction, the solvent was evaporated under reduced pressure. The resulted residue was purified by silica gel column chromatography with CH<sub>2</sub>Cl<sub>2</sub>/MeOH (v/v 100:1) to afford dark red solid as compound **4** (102 mg, 49%).

<sup>1</sup>H NMR (400 MHz, DMSO-*d*<sub>6</sub>) δ 12.35 (s, 1H), 7.77 (t, *J* = 9.6 Hz, 1H), 7.54 (dt, *J* = 19.2, 9.9 Hz, 5H), 7.17 (dd, *J* = 33.5, 9.6 Hz, 2H), 6.79 (d, *J* = 9.9 Hz, 1H), 6.27 (s, 1H), 5.28 (s, 2H), 2.95 (t, *J* = 6.8 Hz, 2H), 2.62 (t, *J* = 6.8 Hz, 2H). <sup>13</sup>C NMR (101 MHz, DMSO-*d*<sub>6</sub>) δ 185.8, 173.0, 162.7, 150.2, 145.8, 145.7, 136.9, 135.6, 135.4, 134.2, 131.8, 129.4, 128.5, 127.8, 114.8, 106.2, 101.7, 70.2, 34.0, 33.9. HRMS: *m/z* [M-H<sup>+</sup>] calculated for C<sub>22</sub>H<sub>16</sub>NO<sub>5</sub>S<sub>2</sub>: 438.0475; measured 438.0473.

**Synthesis of 6.** Resorcinol (10 g, 90.8 mmol), Ethyl 4-Chloroacetoacetate (14.9 g, 90.8 mmol) was dissolved absolutely in ethanol. Zinc chloride (18.5 g, 136 mmol) was added. The mixture was heated and reflux for 12 hours. After complete reaction, cooled to room temperature. The cooled reaction mixture was poured into 100 mL of 0.1 N aqueous hydrochloride acid. Then, the solvent was evaporated under reduced pressure. The resulted residue was purified by silica gel column chromatography with CH<sub>2</sub>Cl<sub>2</sub>/MeOH (v/v 100:1) to afford white solid as compound **6** (11 g, 86%).

<sup>1</sup>H NMR (400 MHz, DMSO-*d*<sub>6</sub>) δ 7.65 (d, *J* = 8.8 Hz, 1H), 6.83 (d, *J* = 6.6 Hz, 1H), 6.75 (s, 1H), 6.40 (s, 1H), 4.92 (s, 2H). <sup>13</sup>C NMR (101 MHz, DMSO-*d*<sub>6</sub>) δ 161.9, 160.6, 155.7, 151.3, 126.9, 113.5, 111.5, 109.8, 102.9, 41.8. HRMS: *m/z* [M+Na]<sup>+</sup> calculated for C<sub>10</sub>H<sub>7</sub>ClNaO<sub>3</sub>: 232.9976; measured 232.9978.

**Synthesis of NC.** Compound **5** was prepared via previous method<sup>25</sup>. Compound **5** (237 mg, 0.95 mmol), Triethylamine (144.7 mg, 1.43 mmol) was dissolved absolutely acetonitrile, compound **6** (281 mg, 0.95 mmol) was added. The mixture was heated and reflux for 24 hours. After complete reaction, cooled to room temperature, the solvent was evaporated under reduced pressure. The resulted residue was purified by silica gel column chromatography with CH<sub>2</sub>Cl<sub>2</sub>/MeOH (v/v 200:1) to afford red solid as compound **NC** (360 mg, 75%).

<sup>1</sup>H NMR (400 MHz, DMSO-*d*<sub>6</sub>) δ 10.55 (s, 1H), 8.49 (d, *J* = 9.1 Hz, 1H), 7.79 (d, *J* = 8.7 Hz, 1H), 6.97 – 6.47 (m, 3H), 6.32 (s, 1H), 4.17 (s, 4H), 3.74 (s, 2H), 2.76 (s, 4H), <sup>13</sup>C NMR (101 MHz, DMSO-*d*<sub>6</sub>) δ 161.6, 160.9, 155.7, 152.7, 145.8, 145.3, 145.3, 136.8, 127.3, 121.7, 113.3, 111.3, 110.7, 104.1, 102.7, 57.6, 52.9, 49.8. HRMS: *m/z* [M+Na]<sup>+</sup> calculated for C<sub>20</sub>H<sub>17</sub>N<sub>5</sub>NaO<sub>6</sub>: 446.1071; measured 446.1075.

**Synthesis of NCR.** Compound **4** (50 mg, 0.11 mmol) was dissolved in anhydrous dichloromethane (5 mL) in a round-bottom flask. **NC** (48.2 mg, 0.11 mmol) was added, followed by the addition of 4-(dimethylamino)-pyridinium-4-toluene sulfonate(DPTS) (33.5 mg, 0.11 mmol) and N, N-Diisopropylcarbodiimide (14.4 mg, 0.11 mmol). The reaction mixture was stirred room temperature. The reaction was monitored by TLC, after complete reaction, diluted with dichloromethane, and washed with brine. The organic layer was dried over anhydrous Na<sub>2</sub>SO<sub>4</sub>, then the solvent was evaporated under reduced pressure. The resulted residue was purified by silica gel column chromatography with CH<sub>2</sub>Cl<sub>2</sub>/MeOH (v/v 150:1) to afford red solid as compound **NCR** (60 mg, 62.5%).

<sup>1</sup>H NMR (400 MHz, CDCl<sub>3</sub>) δ 8.31 (d, *J* = 8.9 Hz, 1H), 7.76 (d, *J* = 8.6 Hz, 1H), 7.58 (dd, *J* = 34.3, 8.4 Hz, 3H), 7.42 – 7.26 (m, 3H), 7.07 – 6.88 (m, 3H), 6.82 – 6.68 (m, 2H), 6.47 (s, 1H), 6.33 – 6.14 (m, 2H), 5.10 (s, 2H), 4.07 (t, *J* = 4.9 Hz, 4H), 3.67 (s, 2H), 3.06 – 2.91 (m, 4H), 2.76 (t, *J* = 5.0 Hz, 4H).

<sup>13</sup>C NMR (101 MHz, CDCl<sub>3</sub>) δ 186.2, 169.5, 162.4, 160.2, 154.5, 152.9, 150.4, 149.7, 145.7, 145.5, 145.0, 144.8, 144.7, 137.3, 135.0, 134.7, 134.6, 134.2, 131.6, 128.5, 128.3, 127.9, 125.6, 118.0, 116.5, 114.8, 114.2, 110.5, 106.7, 102.9, 101.1, 70.3, 58.6, 52.9, 49.3, 33.9, 32.9.

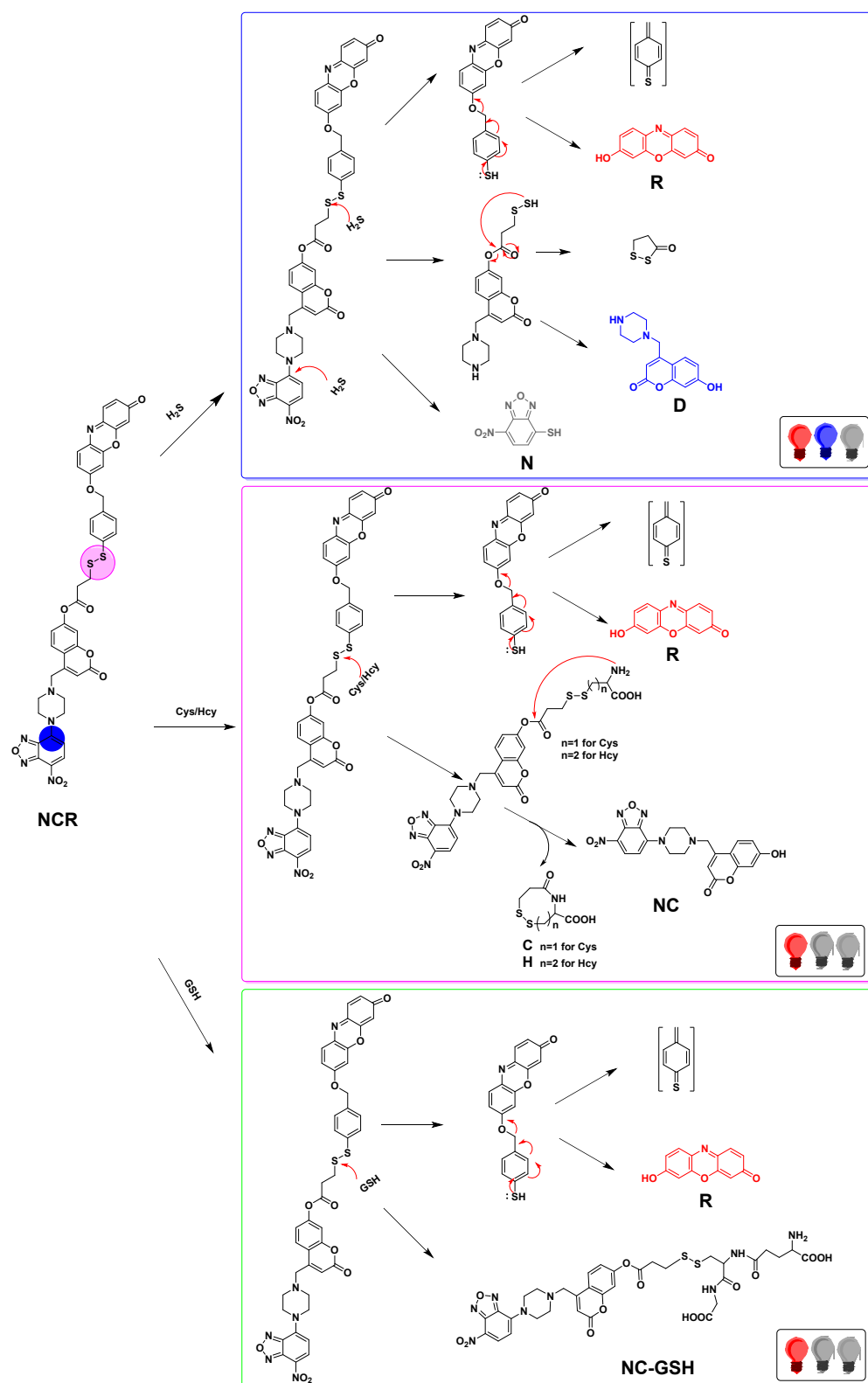
HRMS: *m/z* [M+Na]<sup>+</sup> calculated for C<sub>42</sub>H<sub>32</sub>N<sub>6</sub>NaO<sub>10</sub>S<sub>2</sub>: 867.1514; measured 867.1518.

## References

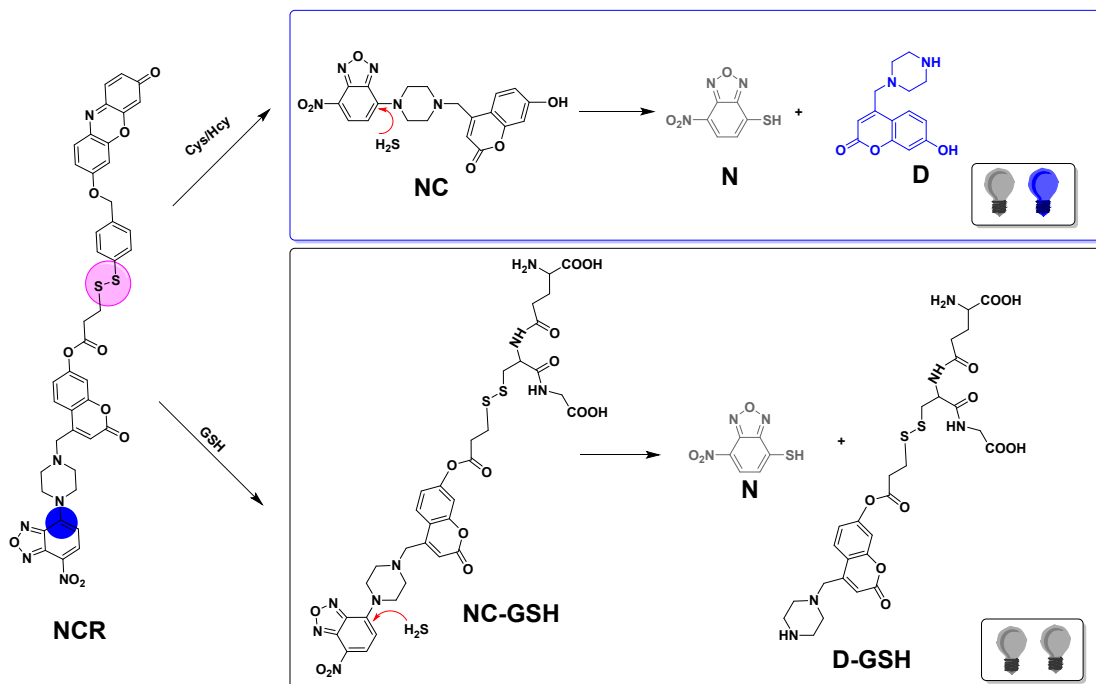
1. (a) L. M. Kiefer and K. J. Kubarych, *J. Phys. Chem. Lett.*, 2016, **7**, 3819-3824;  
(b) G. Hummer, L. R. Pratt and A. E. García, *J. Am. Chem. Soc.*, 1997, **119**, 8523-8527.
2. E. Torres and G. A. DiLabio, *J. Phys. Chem. Lett.*, 2012, **3**, 1738-1744.
3. (a) K. Raghavachari and G. W. Trucks, *J. Chem. Phys.*, 1989, **91**, 1062-1065;  
(b) P. J. Hay, *J. Chem. Phys.*, 1977, **66**, 4377-4384; (c) A. Austin, G. A. Petersson, M. J. Frisch, F. J. Dobek, G. Scalmani and K. Throssell, *J. Chem. Theory Comput.*, 2012, **8**, 4989-5007.
4. H. Lv, X. F. Yang, Y. Zhong, Y. Guo, Z. Li and H. Li, *Anal. Chem.*, 2014, **86**, 1800-1807.
5. H. Li, W. Peng, W. Feng, Y. Wang, G. Chen, S. Wang, S. Li, H. Li, K. Wang and J. Zhang, *Chem. Commun. (Camb.)*, 2016, **52**, 4628-4631.
6. J. Liu, Y.-Q. Sun, H. Zhang, Y. Huo, Y. Shi and W. Guo, *Chem. Sci.*, 2014, **5**, 3183.
7. X. Dai, Z. Y. Wang, Z. F. Du, J. Cui, J. Y. Miao and B. X. Zhao, *Anal. Chim. Acta*, 2015, **900**, 103-110.
8. Y. Li, W. Liu, P. Zhang, H. Zhang, J. Wu, J. Ge and P. Wang, *Biosens. Bioelectron.*, 2017, **90**, 117-124.
9. H. Zhang, R. Liu, J. Liu, L. Li, P. Wang, S. Q. Yao, Z. Xu and H. Sun, *Chem. Sci.*, 2016, **7**, 256-260.
10. J. Liu, Y. Q. Sun, Y. Huo, H. Zhang, L. Wang, P. Zhang, D. Song, Y. Shi and W. Guo, *J. Am. Chem. Soc.*, 2014, **136**, 574-577.
11. Q. Miao, Q. Li, Q. Yuan, L. Li, Z. Hai, S. Liu and G. Liang, *Anal. Chem.*, 2015, **87**, 3460-3466.
12. Y. Yue, F. Huo, P. Ning, Y. Zhang, J. Chao, X. Meng and C. Yin, *J. Am. Chem. Soc.*, 2017, **139**, 3181-3185.
13. X. Li, F. Huo, Y. Yue, Y. Zhang and C. Yin, *Sensors Actuators B: Chem.*, 2017, **253**, 42-49.
14. S. Ding and G. Feng, *Sensors Actuators B: Chem.*, 2016, **235**, 691-697.
15. J. Liu, Y.-Q. Sun, H. Zhang, Y. Huo, Y. Shi, H. Shi and W. Guo, *RSC Adv.*, 2014, **4**, 64542-64550.

16. L. Y. Niu, Y. S. Guan, Y. Z. Chen, L. Z. Wu, C. H. Tung and Q. Z. Yang, *J. Am. Chem. Soc.*, 2012, **134**, 18928-18931.
17. Y. Q. Sun, J. Liu, H. Zhang, Y. Huo, X. Lv, Y. Shi and W. Guo, *J. Am. Chem. Soc.*, 2014, **136**, 12520-12523.
18. S. Y. Lim, K. H. Hong, D. I. Kim, H. Kwon and H. J. Kim, *J. Am. Chem. Soc.*, 2014, **136**, 7018-7025.
19. W. Chen, H. Luo, X. Liu, J. W. Foley and X. Song, *Anal. Chem.*, 2016, **88**, 3638-3646.
20. Q. Hu, C. Yu, X. Xia, F. Zeng and S. Wu, *Biosens. Bioelectron.*, 2016, **81**, 341-348.
21. L. He, X. Yang, K. Xu, X. Kong and W. Lin, *Chem. Sci.*, 2017, **8**, 6257-6265.
22. Y. Li, W. Liu, H. Zhang, M. Wang, J. Wu, J. Ge and P. Wang, *Chem. Asian. J.*, 2017, **12**, 2098-2103.
23. G. X. Yin, T. T. Niu, Y. B. Gan, T. Yu, P. Yin, H. M. Chen, Y. Y. Zhang, H. T. Li and S. Z. Yao, *Angew. Chem. Int. Ed.*, 2018, **57**, 4991-4994.
24. T. Sun, A. Morger, B. Castagner and J. C. Leroux, *Chem. Commun. (Camb.)*, 2015, **51**, 5721-5724.
25. Y. Tang and G.-F. Jiang, *New J. Chem.*, 2017, **41**, 6769-6774.

## 9. Proposed responding mechanism



**Scheme S2.** Proposed responding mechanism of probe **NCR** for simultaneously distinguishing  $\text{H}_2\text{S}$  and biothiols.



**Scheme S3.** Proposed reaction mechanism of NCR pre-treated with Cys, Hcy and GSH upon continued addition of H<sub>2</sub>S.

## 10. Supplementary Spectra

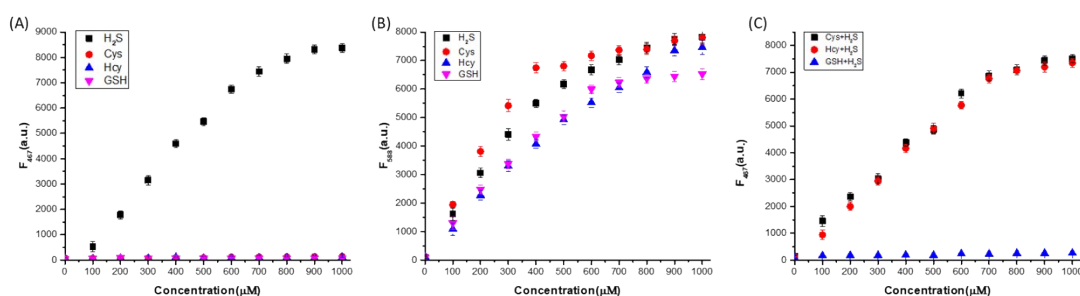


**Fig. S1.** The fluorescence intensity of NCR (10  $\mu$ M) at (A) 467 nm, (B) 588 nm, upon addition of H<sub>2</sub>S (0–100 equiv.), Cys (0–100 equiv.), Hcy (0–100 equiv.) and GSH (0–100 equiv.) and (C) 467 nm pretreated with Cys (100 equiv.), Hcy (100 equiv.), and GSH (100 equiv.) upon continued addition of H<sub>2</sub>S (0–100 equiv.) in DMSO/PBS buffer (25 mM, pH 7.4, 1:99, v/v).  $\lambda_{\text{ex}} = 380$  nm,  $\lambda_{\text{em}} = 467$  nm for the first and third column.  $\lambda_{\text{ex}} = 560$  nm,  $\lambda_{\text{em}} = 588$  nm for the second column. Data are expressed as mean  $\pm$  SD of five parallel experiments.

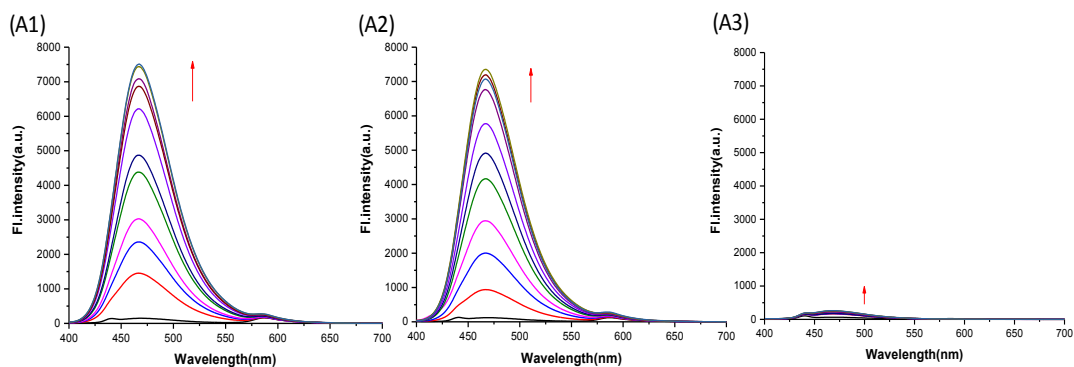


**Fig. S2.** The fluorescence spectra of **NCR** (10  $\mu\text{M}$ ) pre-treated with Cys (100 equiv.), Hcy (100 equiv.), and GSH (100 equiv.) upon continued addition of  $\text{H}_2\text{S}$  (0-100 equiv.) in DMSO/PBS buffer (25 mM, pH 7.4, 1:99, v/v).  $\lambda_{\text{ex}} = 380 \text{ nm}$ ,  $\lambda_{\text{em}} = 467 \text{ nm}$ . Upon continuing addition of increasing amount of  $\text{H}_2\text{S}$  to the mixture of **NCR** (10  $\mu\text{M}$ ) and Cys (100 equiv.), a significant emission centered at 467 nm (50-fold) was generated. A similar phenomenon also occurred in the mixture of **NCR** and Hcy (60-fold). However, the mixture of **NCR** and GSH has no obvious emission band at 467 nm (4-fold).

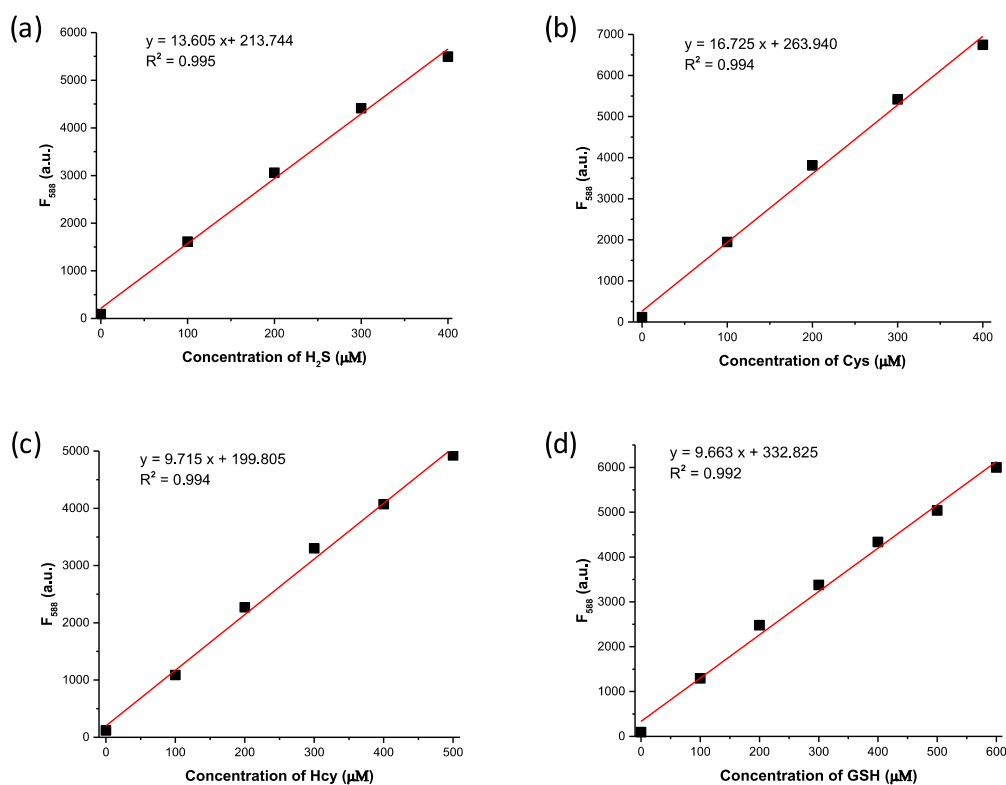


**Fig. S3.** Linear correlation between the fluorescence emission intensity of **NCR** (10  $\mu\text{M}$ ) and (a)  $\text{H}_2\text{S}$  (0 - 40 equiv.), (b) Cys (0 - 40 equiv.), (c) Hcy (0 - 50 equiv.) and (d) GSH (0 - 60 equiv.) in DMSO/PBS buffer (25 mM, pH 7.4, 1:99, v/v).

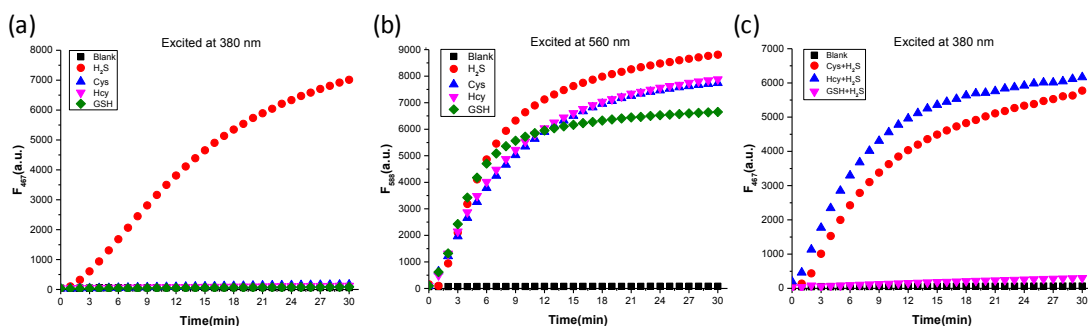


**Fig. S4.** Time-dependent fluorescence spectra of **NCR** (10  $\mu\text{M}$ ) in the presence of Cys (100 equiv.), Hcy (100 equiv.), GSH (100 equiv.),  $\text{H}_2\text{S}$  (100 equiv.) within 30 min in DMSO/PBS buffer (25 mM, pH 7.4, 1:99, v/v). (a) Fluorescence intensity at 467 nm, excitation at 380 nm; (b) Fluorescence intensity at 588 nm, excitation at 560 nm; (c) The fluorescence spectra of **NCR** (10  $\mu\text{M}$ ) pre-treated with 100 equiv. Cys /Hcy and GSH upon continued addition of  $\text{H}_2\text{S}$  (100 equiv.) within 30 min in DMSO/PBS buffer (25 mM, pH 7.4, 1:99, v/v). Fluorescence intensity at 467 nm, excitation at 380 nm.

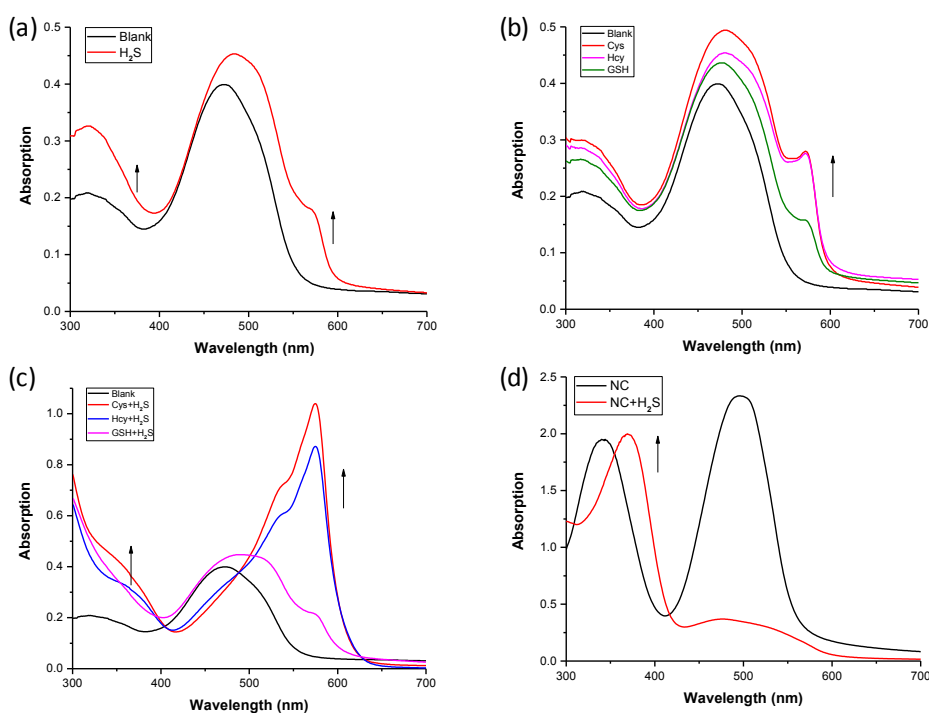
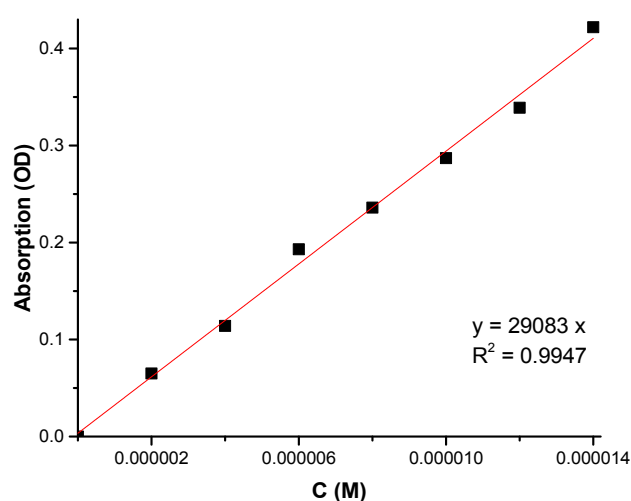


**Fig. S5.** Absorption spectra of (a) **NCR** (10  $\mu\text{M}$ ) in the presence of 100 equiv. of  $\text{H}_2\text{S}$ . (b) **NCR** (10  $\mu\text{M}$ ) in the presence of 100 equiv. of Cys/Hcy and GSH. (c) **NCR** (10  $\mu\text{M}$ ) was pretreated with 100 equiv. Cys/Hcy/GSH in the presence of 100 equiv. of  $\text{H}_2\text{S}$ . (d) **NC** (20  $\mu\text{M}$ ) in the presence of 100 equiv. of  $\text{H}_2\text{S}$  in DMSO/PBS buffer (25 mM, pH 7.4, 1:99, v/v). The UV-vis spectra of free **NCR** showed a main absorption at 475



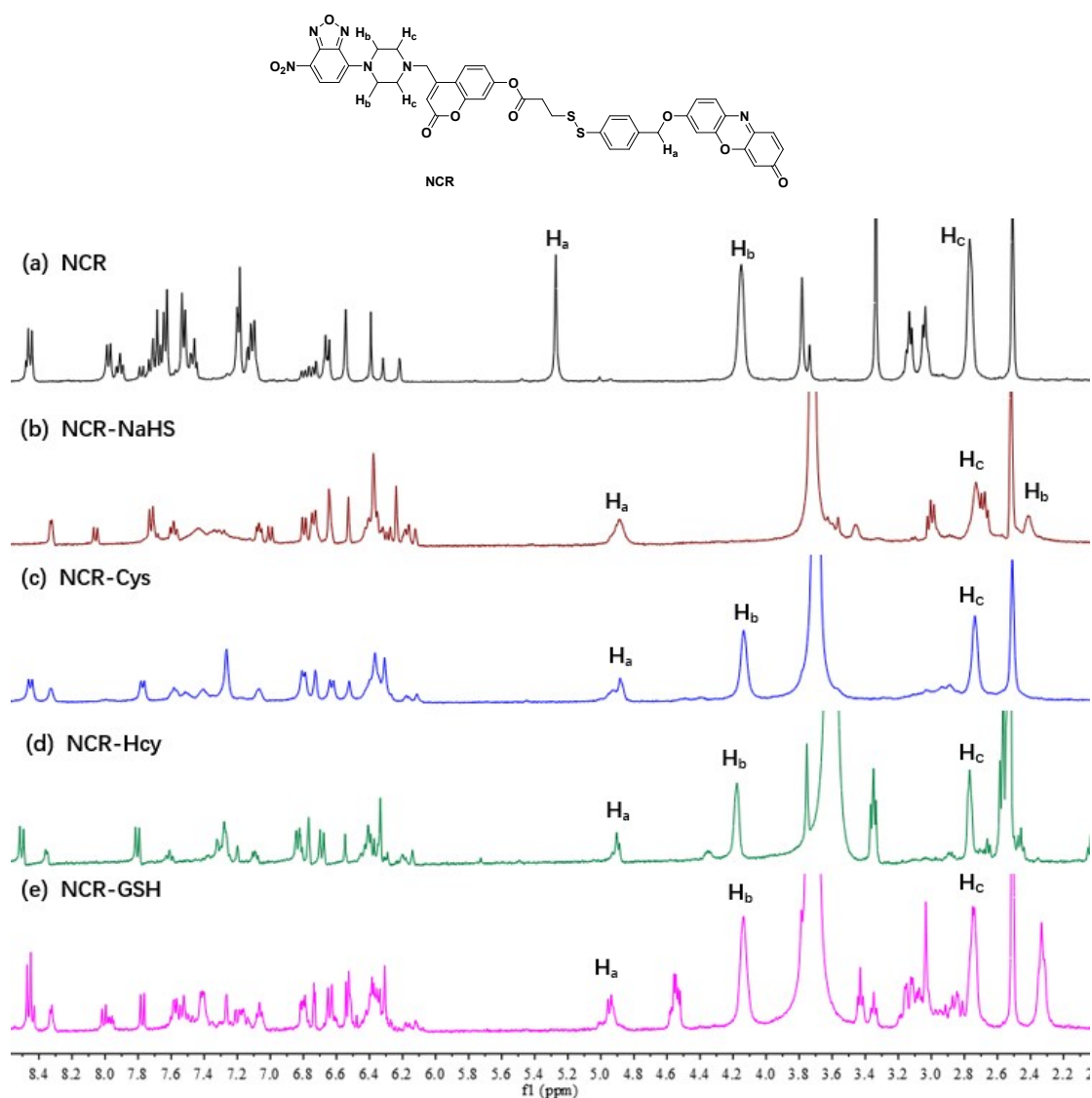
nm. Upon addition of H<sub>2</sub>S, an obvious increase was observed at 372 nm and a shoulder peak simultaneously emerged at 575 nm. These can be attributed to the products **R**, **D** and **N**. Similarly, only an obvious shoulder peak was observed at 575 nm in the presence of Cys/Hcy and GSH. After **NCR** was pre-treated with Cys, Hcy, or GSH (100 equiv.) individually, addition of H<sub>2</sub>S resulted in a significant increase in the UV absorption at 372 nm and the simultaneous emergence of a peak at 575 nm in the Cys- and Hcy-pretreated solutions. However, H<sub>2</sub>S addition only resulted in a shoulder peak at 575 nm for the GSH-pretreated solution. To confirm the original attribution of those newly generated absorption peaks, the absorption spectra of control compounds **NC** and **NC** in the presence of H<sub>2</sub>S were studied, and the results were consistent with the spectral performance of **NCR**.

Extinction coefficient calculations:

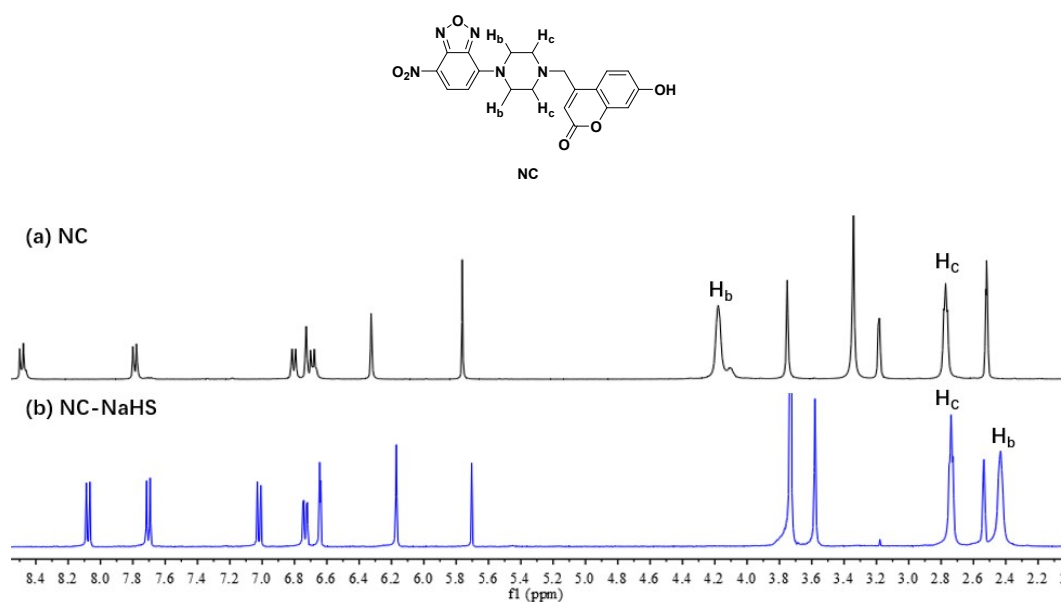


**Fig. S6.** Linear plots of **NCR**. The experiments were applied in 1 cm cuvette, at the indicated concentrations in DMSO/PBS buffer (25 mM, pH 7.4, 1:99 v/v). The measurements were performed at the maximum wavelength of **NCR** (475 nm).

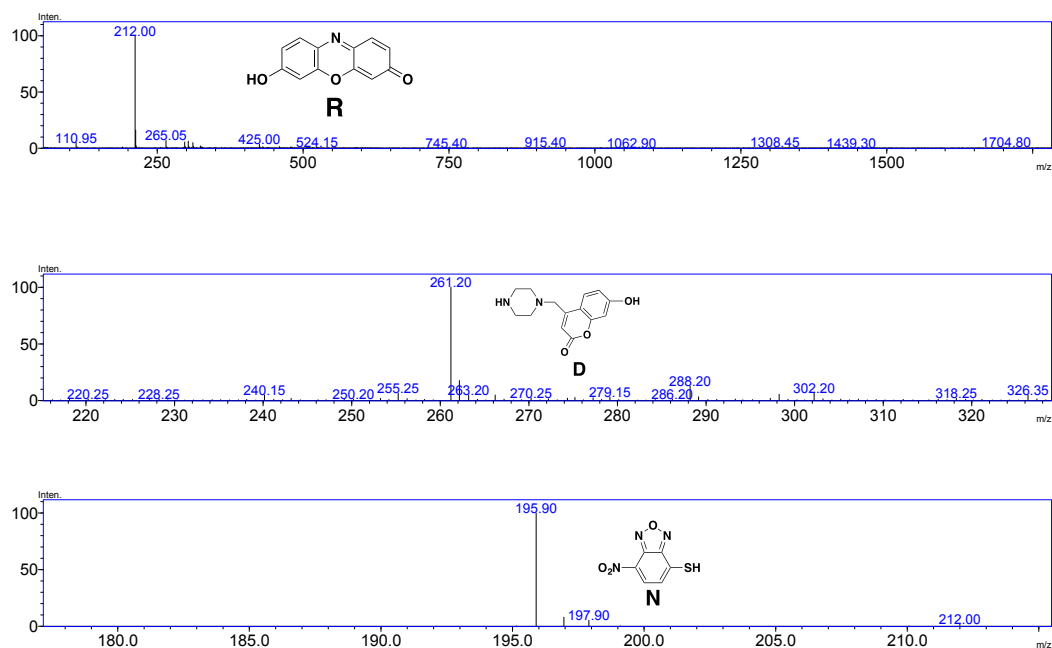
$$\epsilon_{\text{NCR}} = 29083[\text{M}^{-1}\text{cm}^{-1}]$$



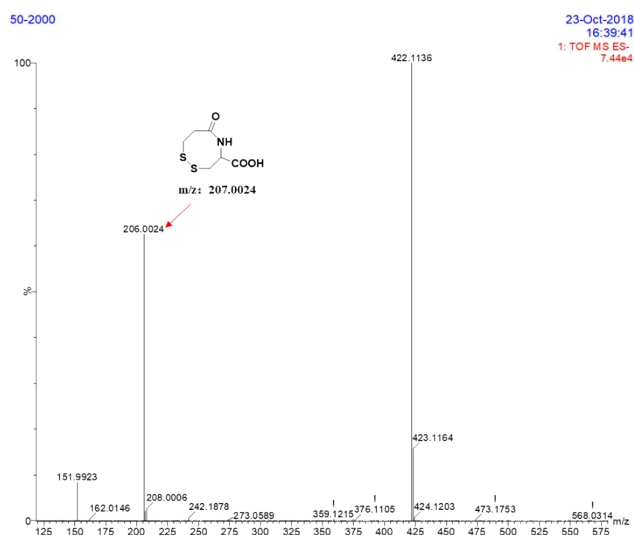
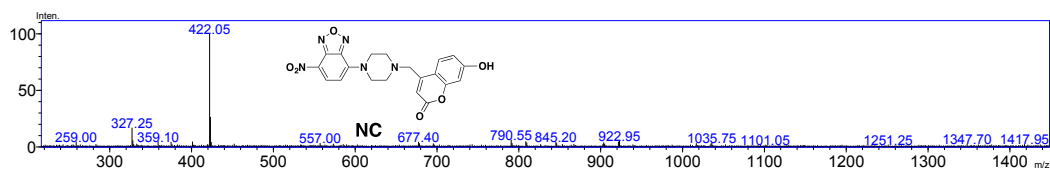
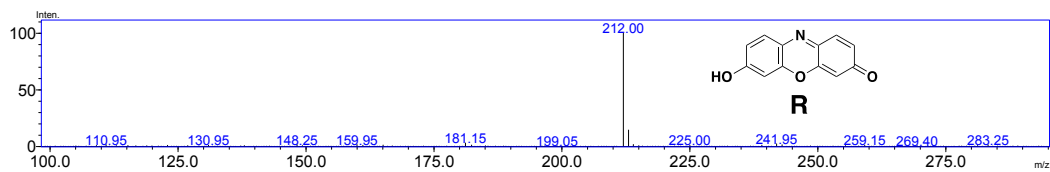
**Fig S7.**  $^1\text{H-NMR}$  spectra comparison: (a) **NCR**, (b) **NCR-NaHS** (c) **NCR-Cys**, (d) **NCR-Hcy** and (e) **NCR-GSH**. The chemical shifts for hydrogens,  $\text{H}_a$  linked with resorufin; and  $\text{H}_c$  linked with coumarin; and  $\text{H}_b$  linked with and NBD were observed during the reaction. In the **NCR-NaHS** group, it was found that the chemical shifts of  $\text{H}_a$  and  $\text{H}_b$  displayed obvious upfield shifts compared with that of **NCR** group, which indicated the release of resorufin and NBD. In **NCR-Cys**, **NCR-Hcy** and **NCR-GSH** group, only upfield shift of  $\text{H}_a$  was observed, but the chemical shift of  $\text{H}_b$  didn't change, which indicated that the release of resorufin, and NBD was not removed (Scheme S2 in supporting information).



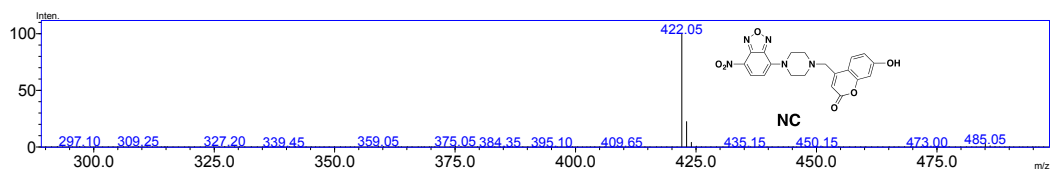
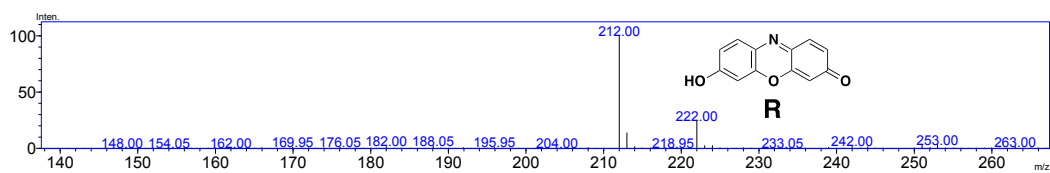
**Fig S8.**  $^1\text{H-NMR}$  spectra comparison of (a) NC and (b) NC-NaHS showed that the chemical shift of  $\text{H}_b$  in NC-NaHS displayed obvious upfield shifts compared with that of NC, which indicated that the NBD was removed (Scheme S3 in supporting information). These results are in good agreement with our proposed reaction mechanism.



**Fig. S9.** Mass spectra (ESI) of NCR in the presence of  $\text{H}_2\text{S}$  in aqueous solution. **R**  $m/z$  ( $M - \text{H}^+$ ) = 212.00, **D**  $m/z$  ( $M + \text{H}^+$ ) = 261.20, **N**  $m/z$  ( $M - \text{H}^+$ ) = 195.90.



**Fig. S10.** Mass spectra of NCR in the presence of Cys in aqueous solution. **R**  $m/z = (M - H^+) = 212.00$ , **NC**  $m/z (M - H^+) = 422.05$ , **C**  $m/z (M - H^+) = 206.0024$ .



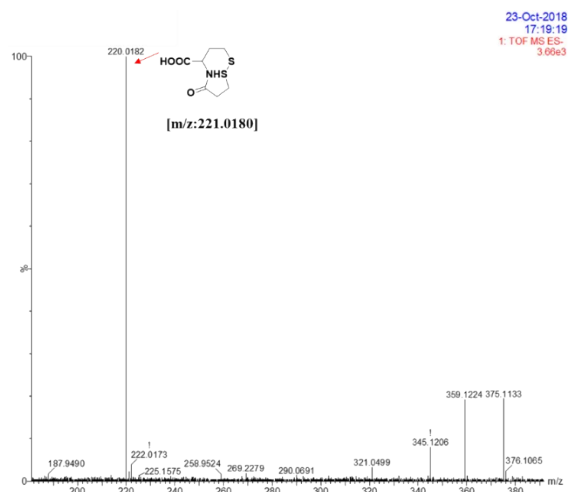


**Fig. S11.** Mass spectra of NCR in the presence of Hcy in aqueous solution. **R**  $m/z = (M - H^+) = 212.00$ , **NC**  $m/z (M - H^+) = 422.05$ , **H**  $m/z (M - H^+) = 220.0182$ .

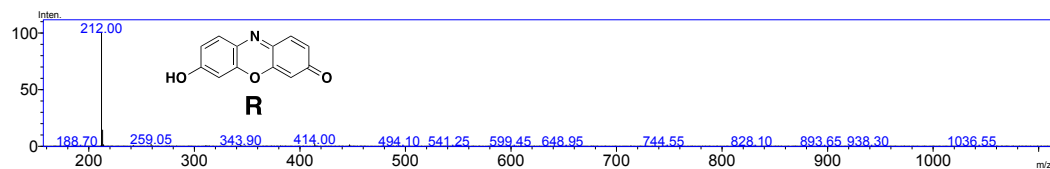
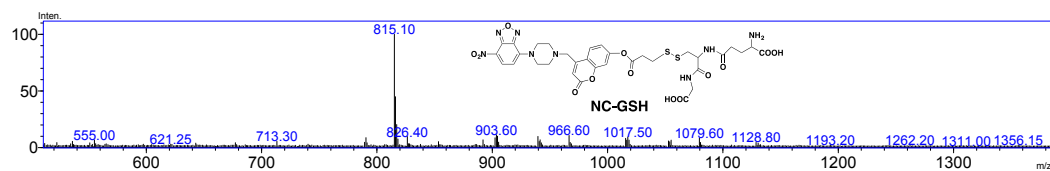


**Fig. S12.** Mass spectra of NCR in the presence of GSH aqueous solution. **R**  $m/z = (M - H^+) = 212.00$ , **NC-GSH**  $m/z (M - H^+) = 815.10$ .

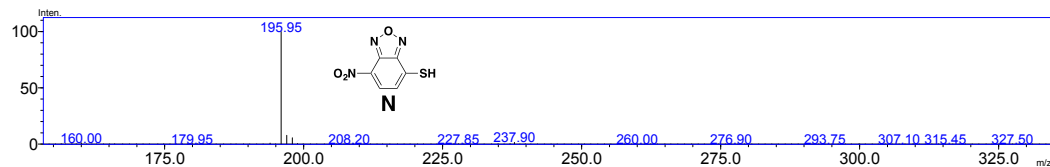
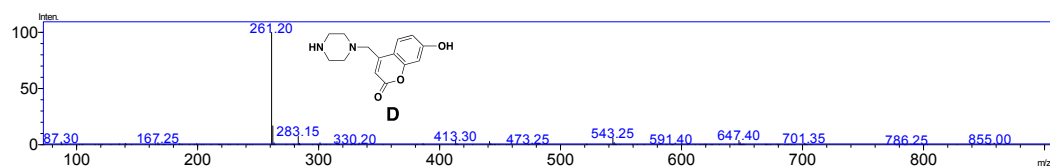


**Fig. S13.** Mass spectra of NCR pre-treated with Cys upon continued addition of  $H_2S$ . **D**  $m/z (M + H^+) = 261.20$ , **N**  $m/z (M - H^+) = 195.95$ .

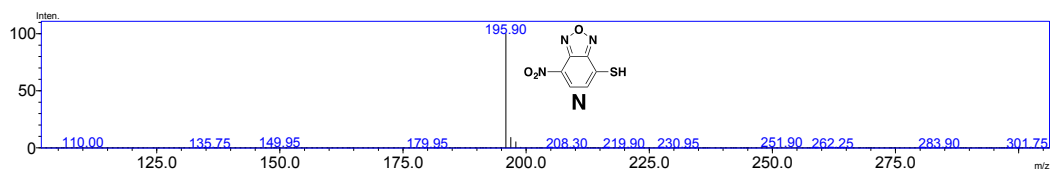
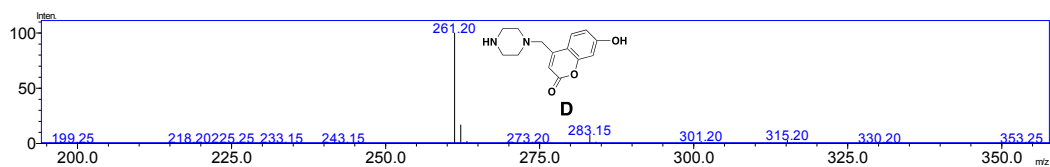


**Fig. S14.** Mass spectra of NCR pre-treated with Hcy upon continued addition of H<sub>2</sub>S. **D**  $m/z$  ( $M + H^+$ ) = 261.20, **N**  $m/z$  ( $M - H^+$ ) = 195.90.

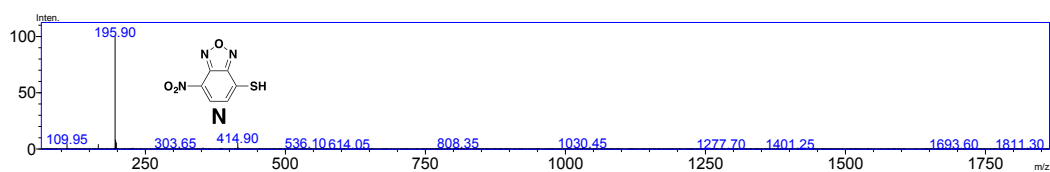
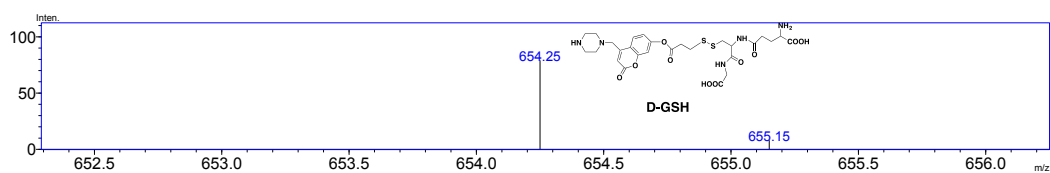


**Fig. S15.** Mass spectra of NCR pre-treated with GSH upon continued addition of H<sub>2</sub>S. **D-GSH**  $m/z$  ( $M + H^+$ ) = 654.25, **N**  $m/z$  ( $M - H^+$ ) = 195.90.

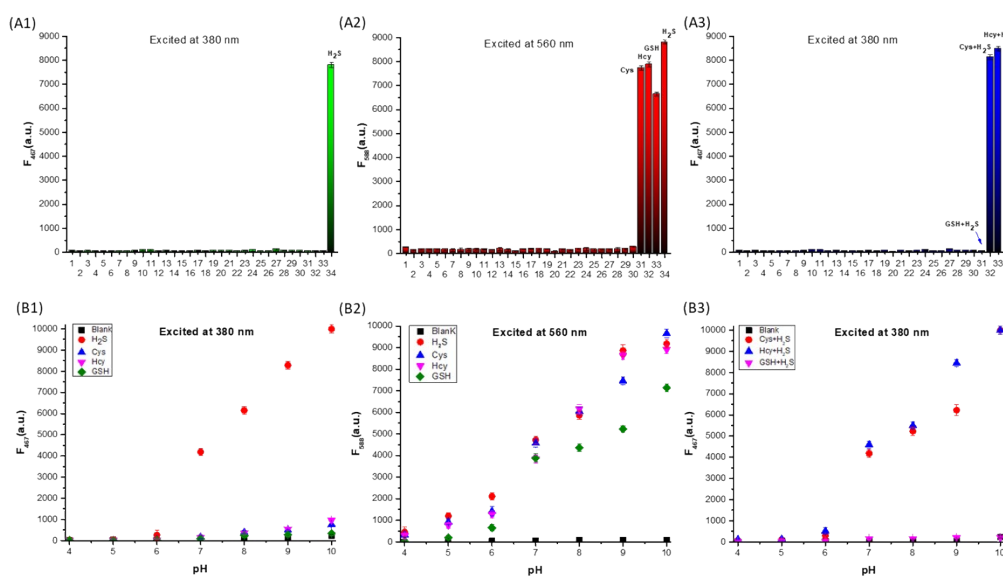
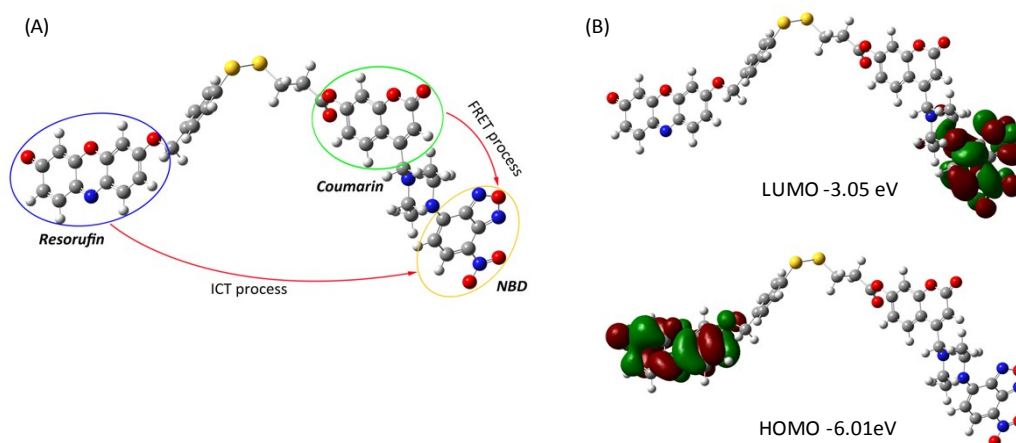


**Fig. S16.** (A) The fluorescence intensity of **NCR** (10  $\mu$ M) at (A1) 467 nm, (A2) 588 nm in the presence of (1) Blank (2) Thr, (3) Phe, (4) Asp, (5) Val, (6) His, (7) Glu, (8) Pro, (9) Met, (10) Ala, (11) Trp, (12) Ser, (13)  $\text{NO}_3^-$ , (14)  $\text{Br}^-$ , (15)  $\text{ClO}^-$ , (16)  $\text{SO}_4^{2-}$ , (17)  $\text{SO}_3^{2-}$ , (18)  $\text{S}_2\text{O}_3^{2-}$ , (19)  $\text{AcO}^-$ , (20)  $\text{N}_3^-$ , (21)  $\text{Ca}^{2+}$ , (22)  $\text{Cu}^{2+}$ , (23)  $\text{Mg}^{2+}$ , (24)  $\text{Fe}^{2+}$ , (25)  $\text{Fe}^{3+}$ , (26)  $\text{Sn}^{2+}$ , (27)  $\text{Zn}^{2+}$ , (28)  $\text{Na}^+$ , (29)  $\text{K}^+$ , (30)  $\text{H}_2\text{O}_2$ , (31) Cys, (32) Hcy, (33) GSH, (34)  $\text{H}_2\text{S}$  in DMSO/PBS buffer (25 mM, pH 7.4, 1:99, v/v). Concentrations were 100 equiv. for (2)–(34). (A3) **NCR** was pre-treated with 100 equiv. (31) Cys (32) Hcy and (33) GSH, upon continued addition of 100 equiv.  $\text{H}_2\text{S}$ . (B). Fluorescence intensity of **NCR** (10  $\mu$ M) at (B1) 467 nm, (B2) 588 nm in the presence or absence of biothiols at different pH values ranging 4.0–10.0 in DMSO/PBS buffer (25 mM, pH 7.4, 1:99, v/v). Concentrations were 100 equiv. for Cys/Hcy, GSH,  $\text{H}_2\text{S}$ . (B3) **NCR** was pre-treated with 100 equiv. Cys/Hcy, GSH, upon continued addition of 100 equiv.  $\text{H}_2\text{S}$ . Excitation at 380 nm for (A1/B1), 560 nm for (A2/B2), and 380 nm for (A3/B3). The results showed the fluorescence intensity of free **NCR** at two emission bands was not influenced by pH in aqueous solutions. However, at pH ranging from 7.0 to 8.0, probe **NCR** generated significant enhancement of the fluorescence intensity in the presence of  $\text{H}_2\text{S}$ , Cys/Hcy and GSH. Data are expressed as mean  $\pm$  SD of five parallel



experiments.

**Fig. S17.** (A) Optimized structures of **NCR** and the co-regulation of response emission by FRET and ICT mechanisms. (B) Frontier molecular orbital energy of **NCR** at the excited state. Calculations were performed using DFT with the B3LYP exchange functional employing 6-31G(d) basis sets using Gaussian 09 programs. In the optimized

structures of **NCR**, the calculated distance between coumarin and NBD is 13 Å. Thus, the FRET donor fluorescence of coumarin can be quenched by the NBD moiety through the FRET process. In addition, the  $\pi$  electrons on both the HOMO and LUMO efficiently distribute in the respective resorufin and NBD units in **NCR**, suggesting that **NCR** is a typical intramolecular charge transfer (ICT)-based fluorescent probe.

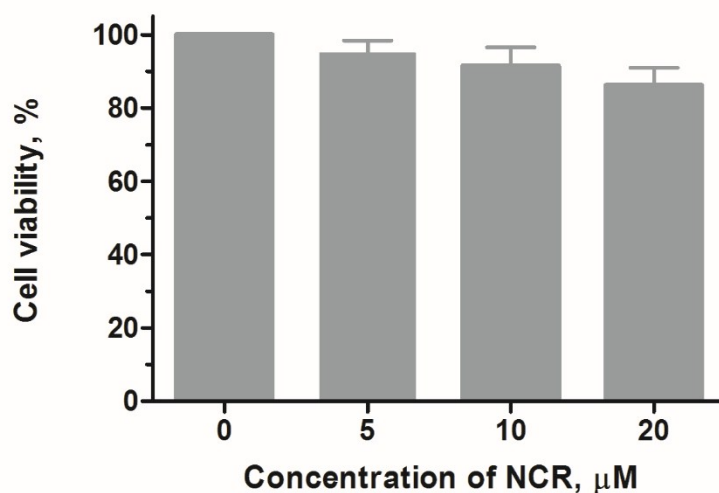


**Fig. S18.** The cell viability of living HeLa cells treated with 5, 10, or 20  $\mu\text{M}$  **NCR** for 24 hours measured by standard MTT assay. (Error bars represent the standard deviations of five trials)

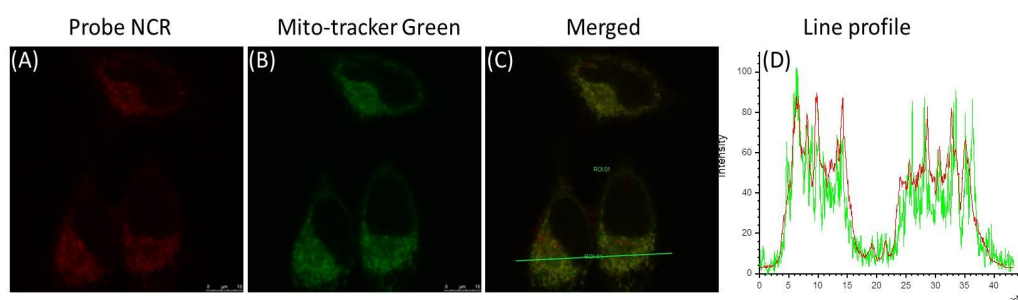


**Fig. S19.** The images of living HeLa cells pre-treated with **NCR** (5  $\mu\text{M}$ ) for 30 min and subsequently co-incubated with Mito-Tracker Green (1  $\mu\text{M}$ ) for 30 min. (A) Red channel images of probe **NCR** ( $\lambda_{\text{ex}} = 561 \text{ nm}$ ,  $\lambda_{\text{em}} = 575 - 620 \text{ nm}$ ); (B) Green channel images of Mito -Tracker Green ( $\lambda_{\text{ex}} = 488 \text{ nm}$ ,  $\lambda_{\text{em}} = 500 - 535 \text{ nm}$ ); (C) Merged green and red channel images; (D) The intensity profile of the ROI in merged images. Scale bar: 10  $\mu\text{m}$ .



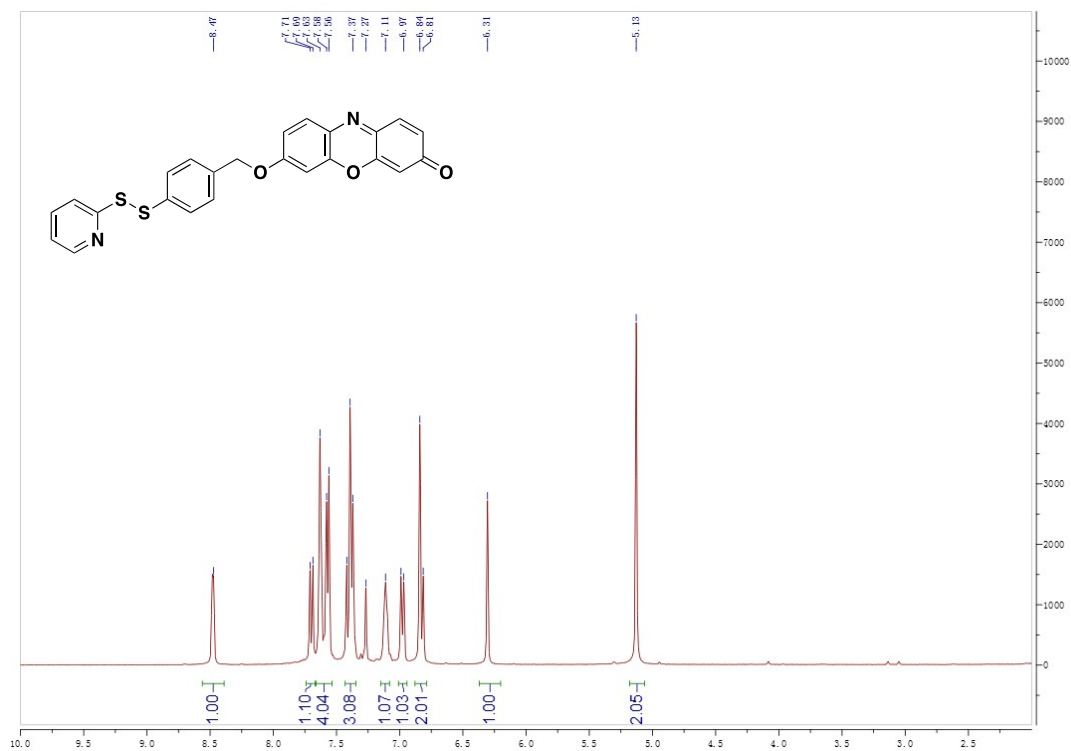


**Fig. S20.**  $^1\text{H}$  NMR of compound **3** in  $\text{CDCl}_3$ .

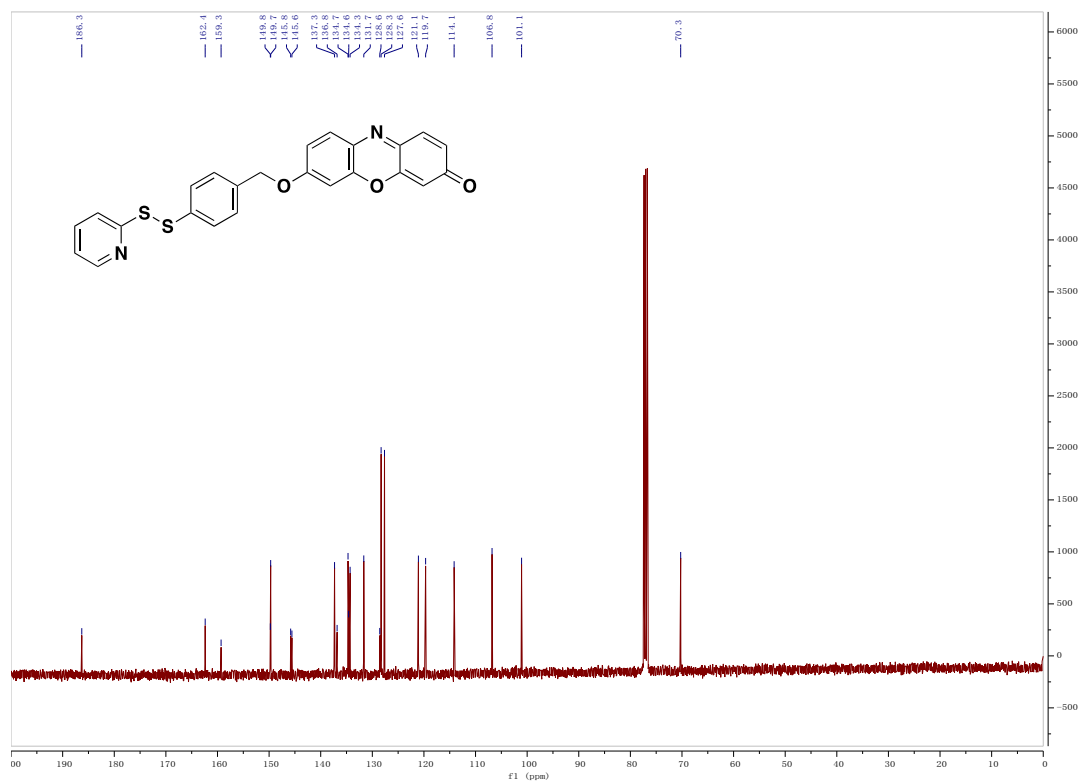


**Fig. S21.**  $^{13}\text{C}$  NMR of compound **3** in  $\text{CDCl}_3$ .

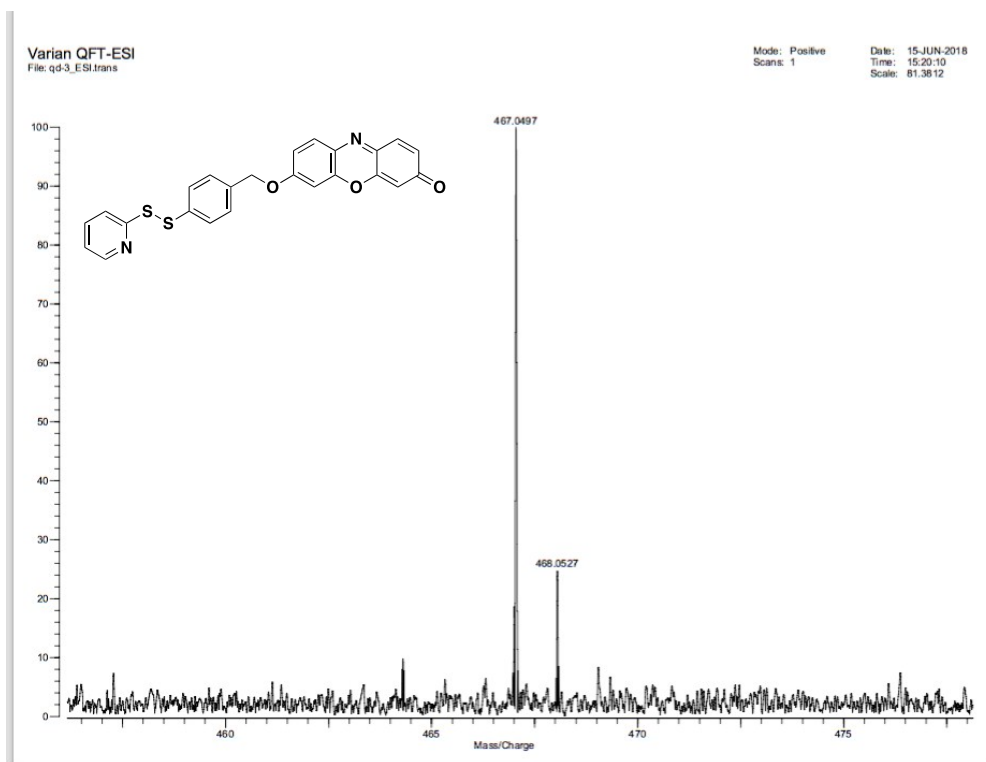


**Fig. S22.** HRMS (ESI) of compound **3**  $m/z$   $[M+Na]^+$  calculated for  $C_{24}H_{16}N_2NaO_3S_2$  : 467.0495; measured 467.0497.

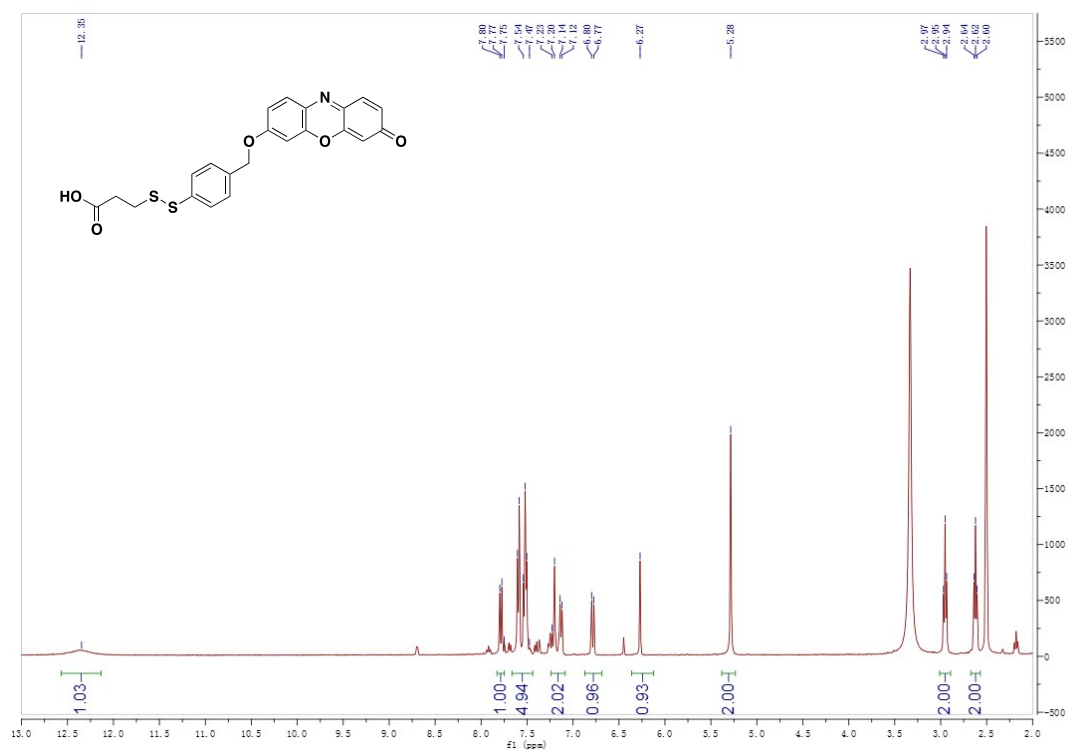


**Fig. S23.**  $^1H$  NMR of compound **4** in  $DMSO-d_6$ .

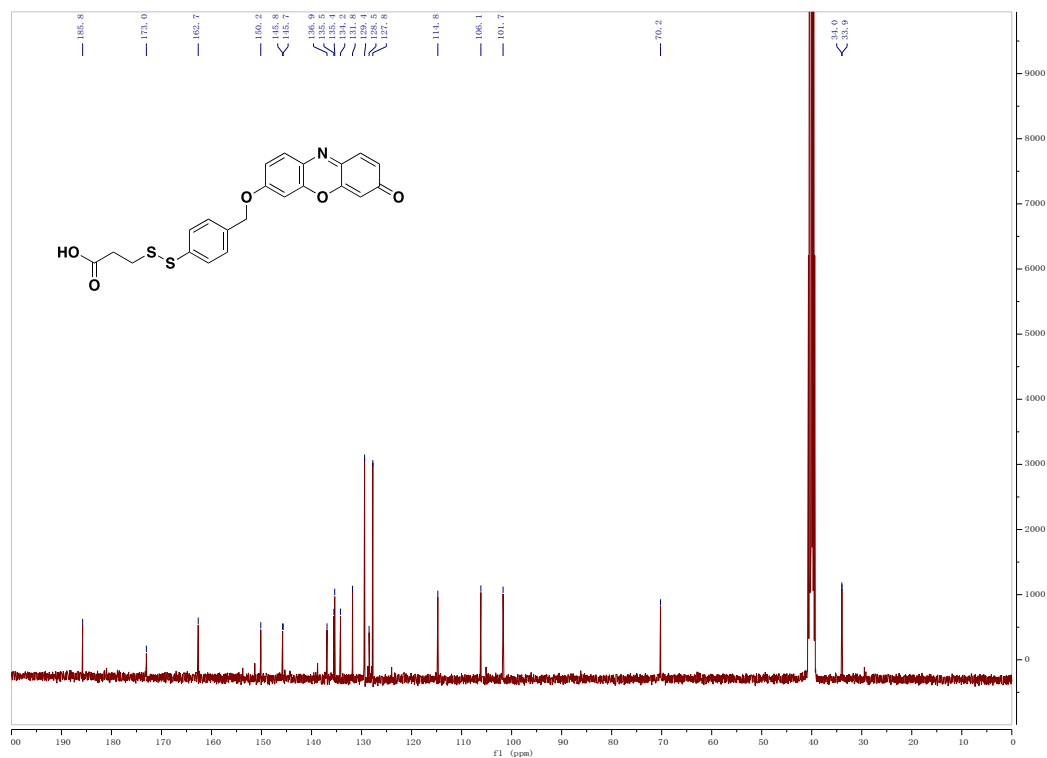


**Fig. S24.**  $^{13}\text{C}$  NMR of compound **4** in  $\text{DMSO-}d_6$ .

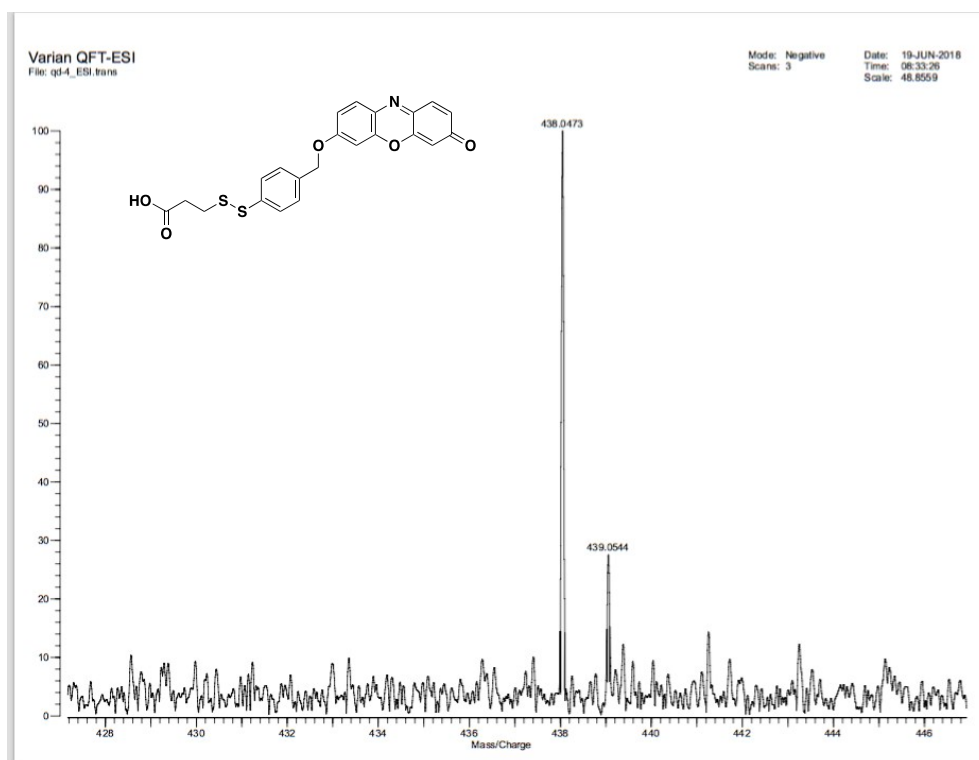


**Fig. S25.** HRMS (ESI) of compound **4**  $m/z$   $[\text{M-H}^+]$  calculated for  $\text{C}_{22}\text{H}_{16}\text{NO}_5\text{S}_2$ : 438.0475; measured 438.0473.

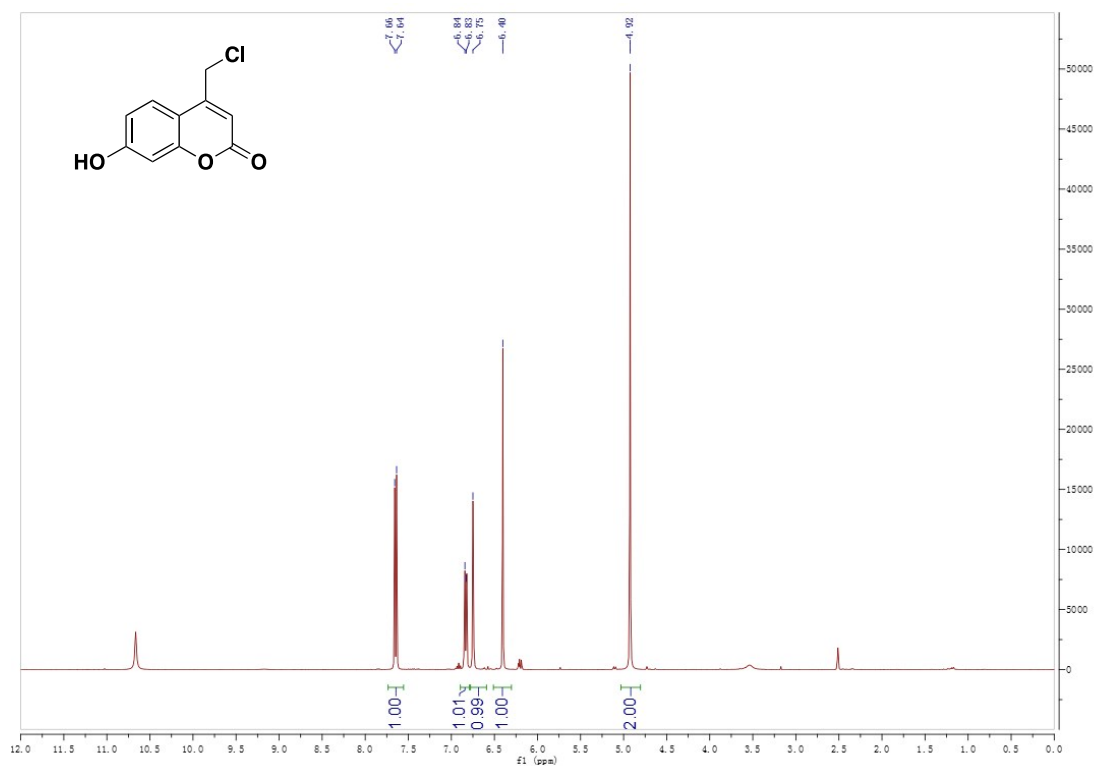


**Fig. S26.** <sup>1</sup>H NMR of compound **6** in DMSO-*d*<sub>6</sub>.

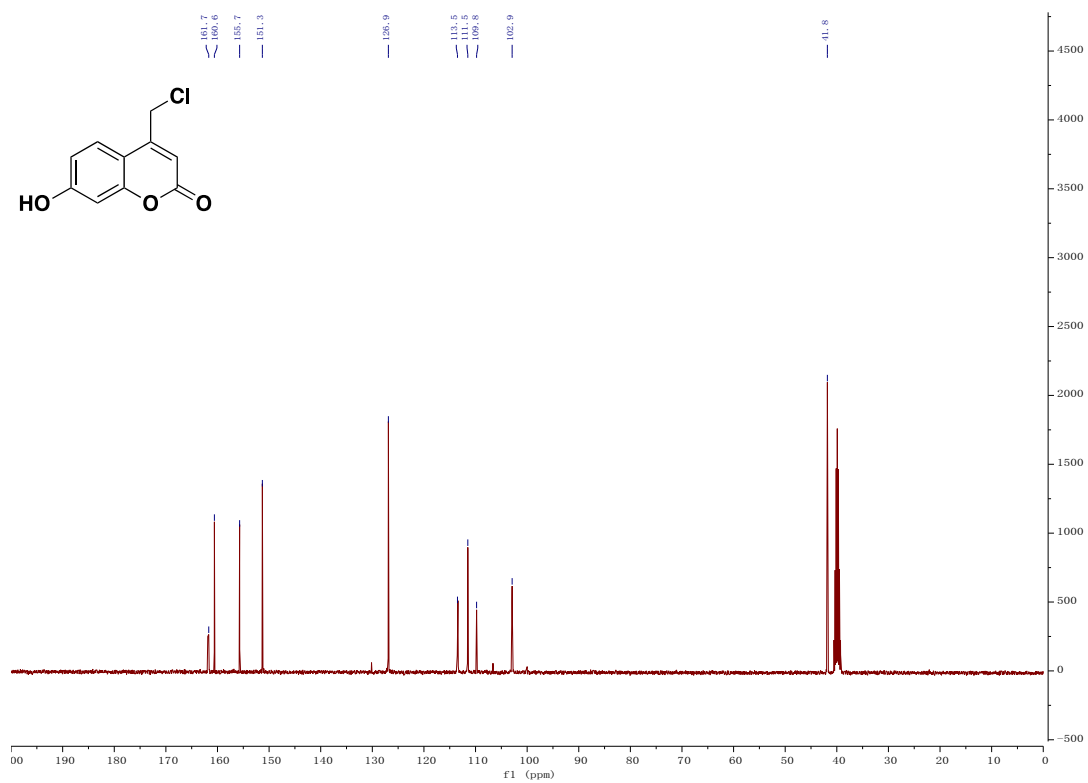


**Fig. S27.** <sup>13</sup>C NMR of compound **6** in DMSO-*d*<sub>6</sub>.

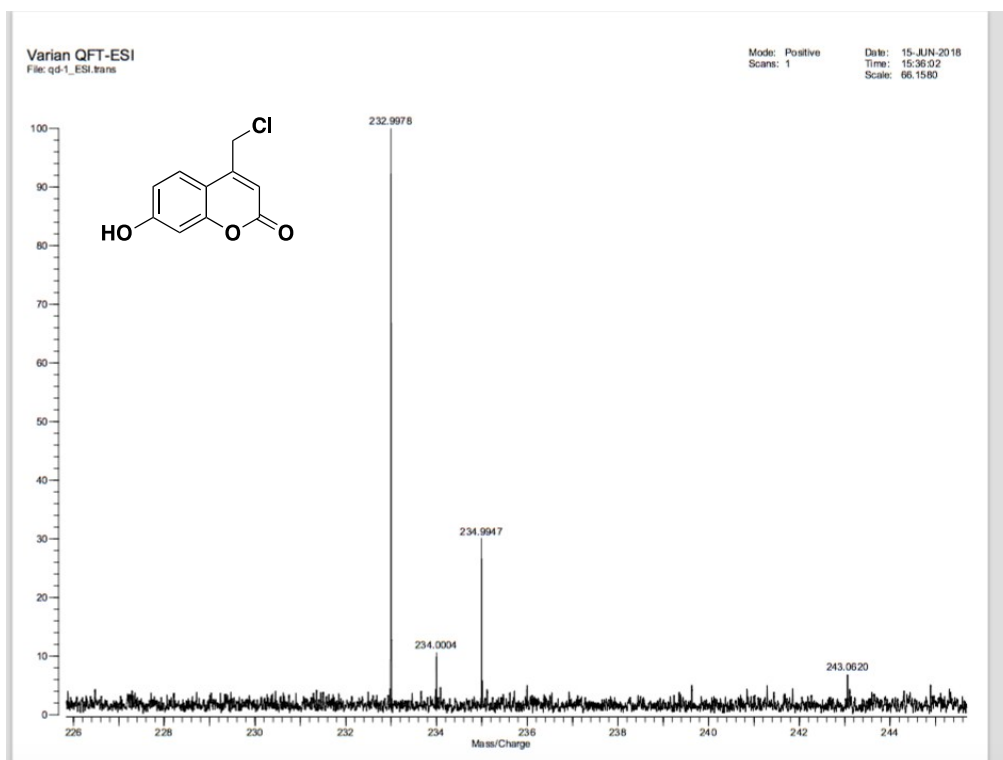


**Fig. S28.** HRMS (ESI) of compound **6**  $m/z$   $[M+Na]^+$  calculated for  $C_{10}H_7ClNaO_3$ : 232.9976; measured: 232.9978.

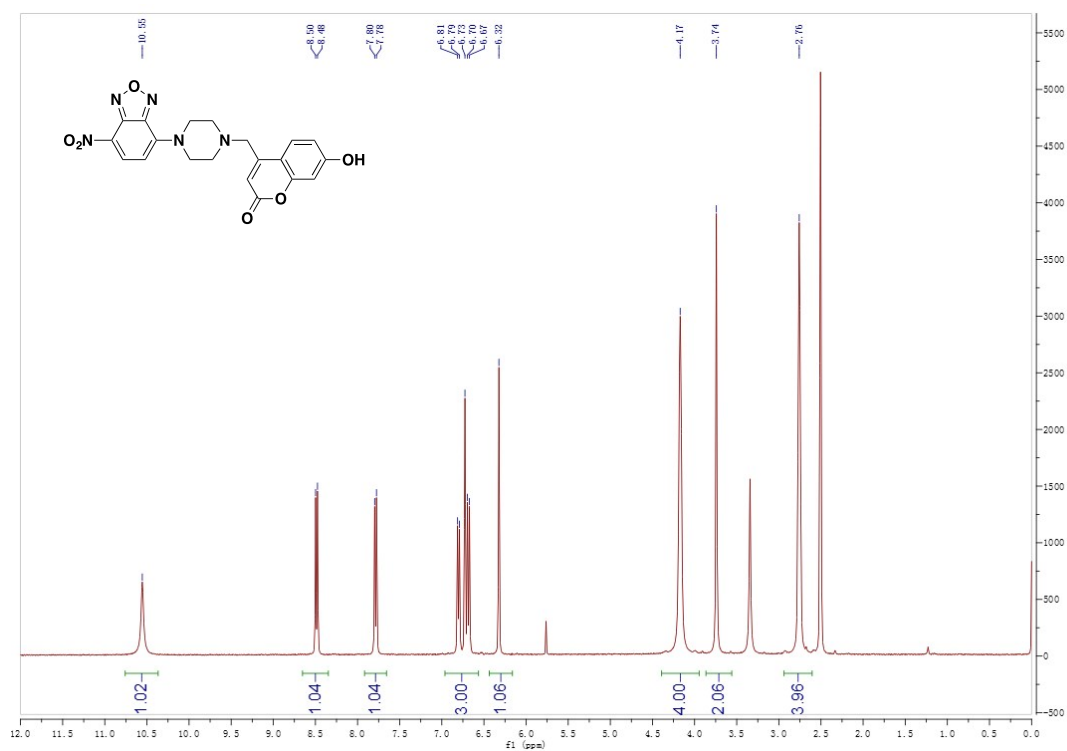


**Fig. S29.**  $^1H$  NMR of compound **NC** in  $DMSO-d_6$ .

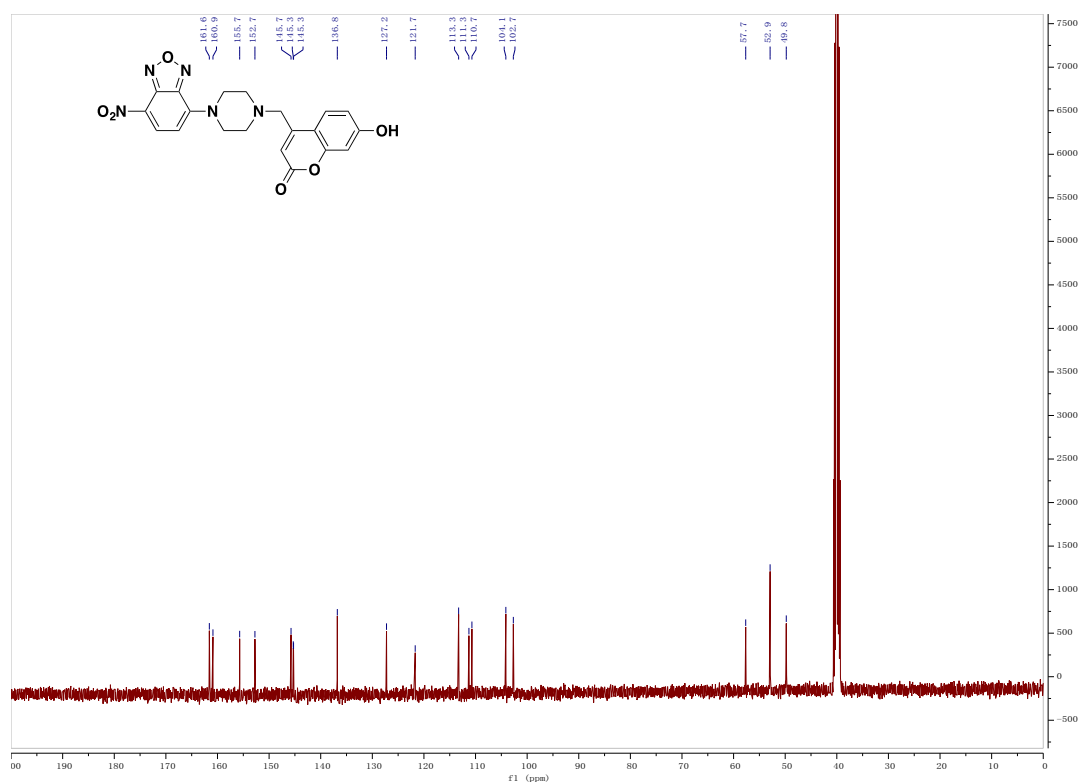


**Fig. S30.**  $^{13}\text{C}$  NMR of compound NC in  $\text{DMSO-}d_6$ .

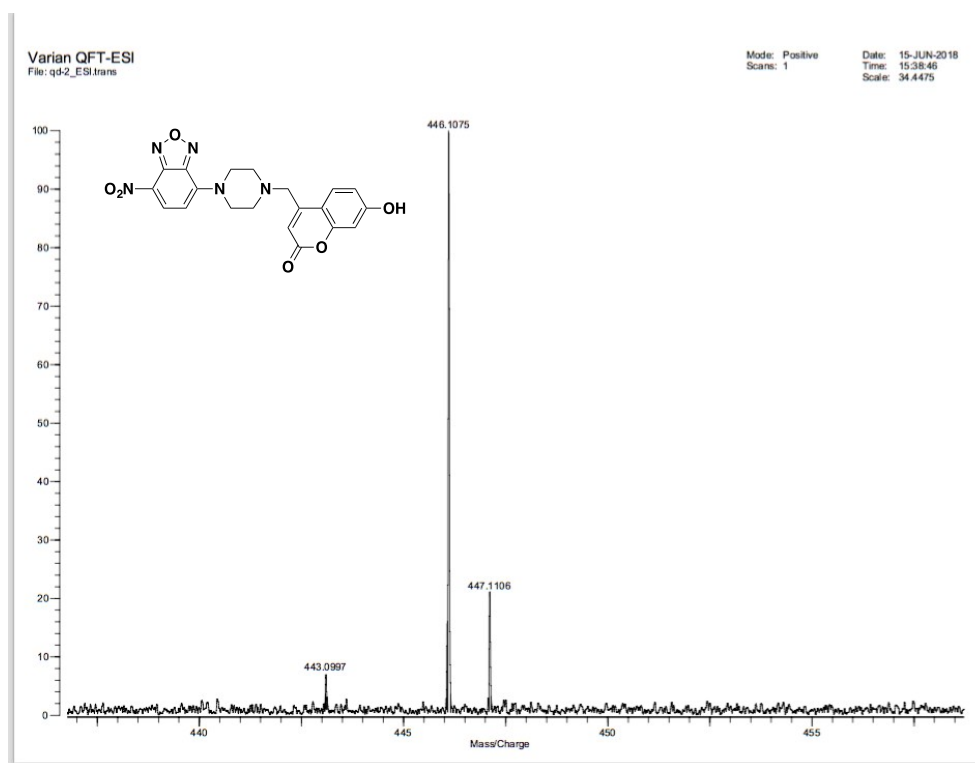


**Fig. S31.** HRMS (ESI) of compound NC  $m/z$   $[\text{M}+\text{Na}]^+$  calculated for  $\text{C}_{20}\text{H}_{17}\text{N}_5\text{NaO}_6$ : 446.1071; measured: 446.1075.

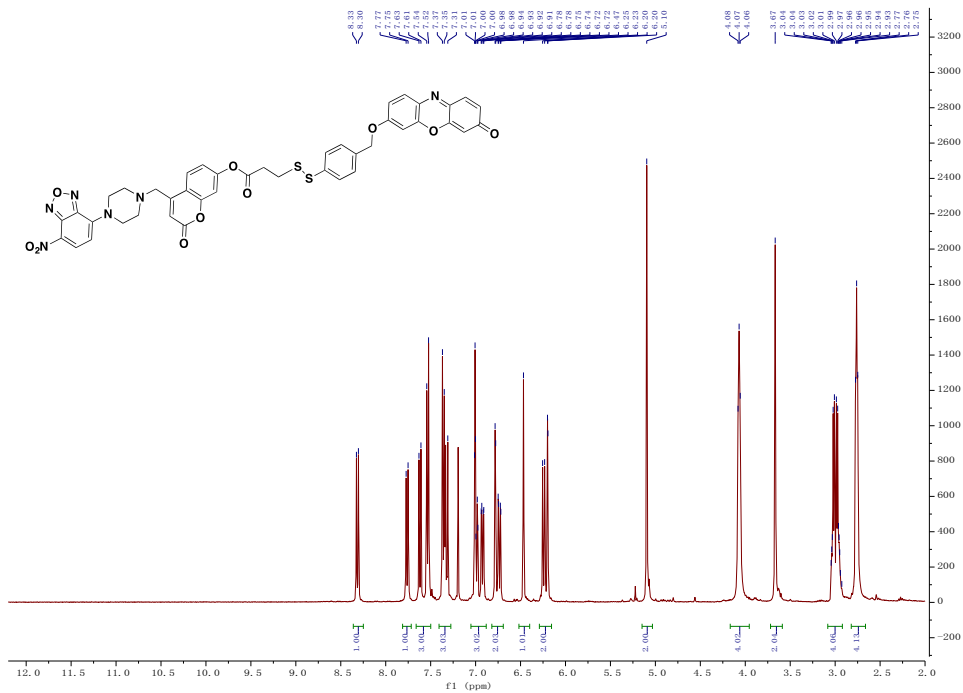


**Fig. S32.**  $^1\text{H}$  NMR of compound NCR in  $\text{CDCl}_3$ .

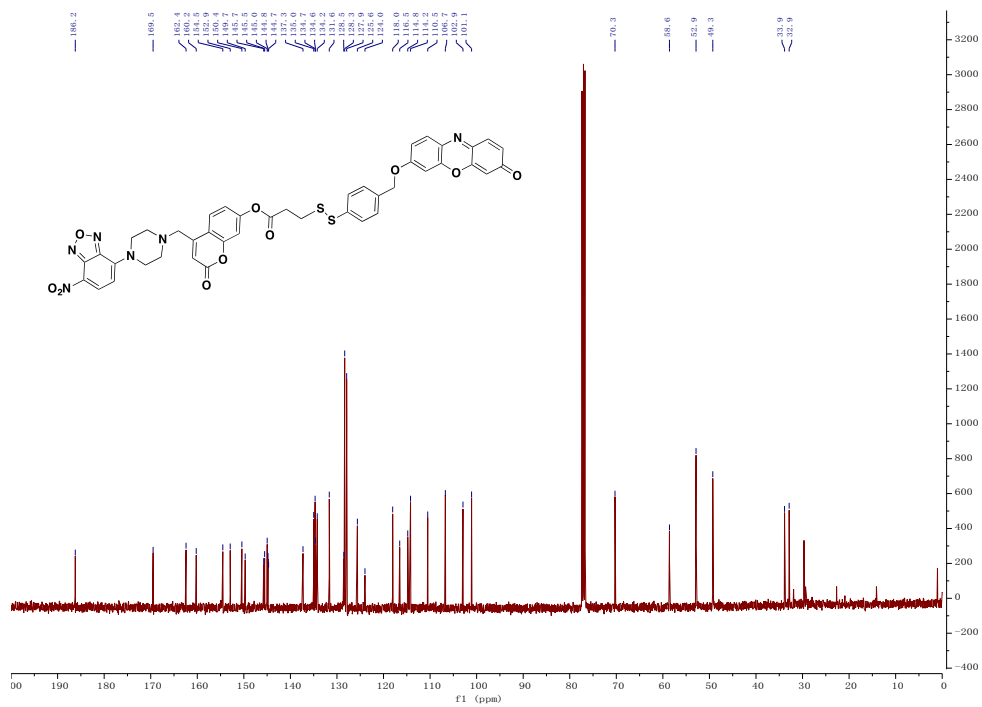


**Fig. S33.**  $^{13}\text{C}$  NMR of compound NCR in  $\text{CDCl}_3$ .

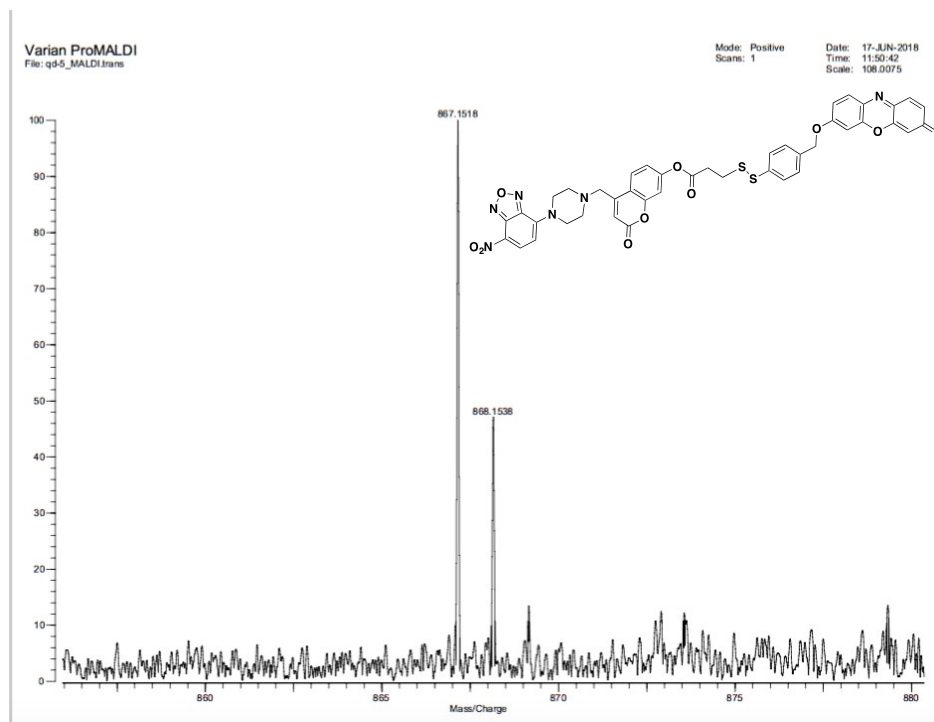


**Fig. S34.** HRMS (ESI) of compound **NCR**  $m/z$   $[M+Na]^+$  calculated for  $C_{42}H_{32}N_6NaO_{10}S_2$ : 867.1514; measured 867.1518.